

Nonequilibrium dynamics in one-dimensional strongly interacting two-component gases

Ovidiu I. Pătu¹

¹*Institute for Space Sciences, Bucharest-Măgurele, R 077125, Romania*

The derivation of determinant representations for the space-, time-, and temperature-dependent correlation functions of the impenetrable Gaudin-Yang model in the presence of a trapping potential is presented. These representations are valid in both equilibrium and nonequilibrium scenarios like the ones initiated by a sudden change of the confinement potential. In the equal-time case our results are shown to be equivalent to a multicomponent generalization of Lenard's formula from which Painlevé transcendent representations for the correlators can be obtained in the case of harmonic trapping and Dirichlet and Neumann boundary conditions. For a system in the quantum Newton's cradle setup the determinant representations allow for an exact numerical investigation of the dynamics and even hydrodynamization which is outside the reach of Generalized Hydrodynamics or other approximate methods. In the case of a sudden change in the trap's frequency, we predict a many-body bounce effect, not present in the evolution of the density profile, which causes a nontrivial periodic narrowing of the momentum distribution with amplitude depending on the statistics of the particles.

I. INTRODUCTION

The study of nonequilibrium phenomena represents one of the most active area of research in modern physics. Due to the unprecedented degree of control over interactions, dimensionality and statistics the field of ultracold gases represents the ideal testing ground for various nonequilibrium scenarios in which isolated many-body systems can be accurately observed [1–3]. One-dimensional (1D) systems are of particular interest as they can realize integrable systems which are experimentally accessible and in which analytical results can verify and complement more general approximate methods. The realization that integrable and near-integrable models in 1D do not thermalize [4, 5], as it was shown in the pioneering quantum Newton's cradle experiment [4], reignited interest in the study of such systems resulting in the introduction of powerful techniques like the Quench Action [6, 7] and Generalized Hydrodynamics [8, 9] (GHD). While initial investigations focused on single component systems in recent years several studies on multicomponent systems, which present a richer phenomenology like spin-charge separation and the spin-incoherent regime, have also appeared in the literature [10–20].

In 1D continuum systems with infinitely repulsive contact interactions (also known as the Tonks-Girardeau regime) the correlation functions can be computed as determinants opening the way for the exact investigation of the dynamics [21]. For periodic boundary conditions and no external potential determinant representations were obtained in Refs. [22–24] for the single component Lieb-Liniger (LL) model and in Refs. [25–27] for the two-component Gaudin-Yang (GY) model. The general case of systems in external trapping potentials has been addressed only recently for the bosonic LL model in [28] and generalized for arbitrary statistics (anyons) in [28–30] (for equal-time correlators similar representations results were derived earlier in the case of harmonic trapping in [31–34] and in rather general nonequilibrium scenarios in [35–38]). In this article we derive determinant representations for the space-, time-, and temperature-dependent correlation functions of the arbitrary statistics Gaudin-Yang model in the presence of a trapping potential which can also depend on time. Our results are valid in both equilibrium and nonequilibrium scenarios which can be realized in current experiments. In the equal-time case we show the equivalence of the determinant representation with a multicomponent generalization of Lenard's formula [22]. Lenard's formula makes transparent the connection between the correlation functions of the GY model and the gap probabilities in certain random matrix ensembles which were previously calculated [39]. In this way Painlevé transcendent representations for the correlators of finite size systems at zero temperature can be easily derived. We also employ our results for the investigation of the dynamics in two experimentally relevant nonequilibrium scenarios: the sudden change in the trap's frequency and the quantum Newton's cradle setup. In the first scenario we discover a collective many-body bounce effect similar with the one described and investigated by Atas *et al.* [40] in the case of single component systems (see also [38]). The effect can be seen in the periodic narrowing of the momentum distribution function (MDF) when the gas is maximally compressed and is not present in noninteracting systems subjected to the same quench. The amplitude of the narrowing is dependent on the statistics. Very recently, the phenomenon of hydrodynamization [41], which describes the rapid onset of hydrodynamics on the fastest available scale in a system quenched with an energy much larger than its ground state energy, has been observed in the LL model [42]. The main feature of hydrodynamization in the QNC setup, the rapid change of energy in the momentum modes between the Bragg peaks, cannot be captured by GHD but it can be accurately monitored using our determinant representation. We perform a

detailed investigation of hydrodynamization in the GY model highlighting the differences between the two-component and single component systems.

The plan of the paper is as follows. In Sec. II we introduce the Gaudin-Yang model, the eigenstates, wavefunctions and the correlators. In Sec. III we present results for the form factors and in Sec. IV the determinant representations for the correlators. The particular case of equal-time correlators and the equivalence with Lenard's formula is described in Secs. V and VI. The dynamics in the case of variable frequency can be found in Sec. VII and the investigation of hydrodynamization is presented in Sec. VIII. We conclude in Sec. IX. Technical details regarding the derivation of the determinant representations, the equivalence with Lenard's formula and the thermodynamics of the trapped GY model can be found in several Appendices.

II. THE ANYONIC GAUDIN-YANG MODEL IN THE PRESENCE OF AN EXTERNAL POTENTIAL

We consider a one-dimensional system of particles with two internal states and infinite repulsive contact interactions in the presence of an external confining potential which can also depend on time. In second quantization the Hamiltonian can be written as

$$H = \int dx \frac{\hbar^2}{2m} \partial_x \Psi^\dagger \partial_x \Psi + g : (\Psi^\dagger \Psi)^2 : + (V(x, t) - \mu) \Psi^\dagger \Psi + B(\Psi^\dagger \sigma_z \Psi), \quad (1)$$

where m is the mass of the particles, $g = \infty$ characterizes the strength of the interaction, $\Psi = (\Psi_\uparrow(x), \Psi_\downarrow(x))^T$, $\Psi^\dagger = (\Psi_\uparrow^\dagger(x), \Psi_\downarrow^\dagger(x))$ and $:$ denotes normal ordering. In (1) μ is the chemical potential, B the magnetic field, σ_z the third Pauli matrix and $\Psi_{\uparrow, \downarrow}(x)$ are anyonic fields satisfying the following commutation relations ($\alpha, \beta \in \{\uparrow, \downarrow\}$):

$$\Psi_\alpha(x) \Psi_\beta^\dagger(y) = -e^{-i\pi\kappa \text{sign}(x-y)} \Psi_\beta^\dagger(y) \Psi_\alpha(x) + \delta_{\alpha, \beta} \delta(x-y), \quad (2a)$$

$$\Psi_\alpha(x) \Psi_\beta(y) = -e^{i\pi\kappa \text{sign}(x-y)} \Psi_\beta(y) \Psi_\alpha(x), \quad (2b)$$

$$\Psi_\alpha^\dagger(x) \Psi_\beta^\dagger(y) = -e^{i\pi\kappa \text{sign}(x-y)} \Psi_\beta^\dagger(y) \Psi_\alpha^\dagger(x), \quad (2c)$$

with $\text{sign}(x) = x/|x|$, $\text{sign}(0) = 0$ and $\kappa \in [0, 1]$ is the statistics parameter (note that an equally valid choice for the statistics parameter could have been $\kappa \in [-1, 0]$). For $x \neq y$, as we vary the statistical parameter the commutation relations (2) interpolate continuously between the ones for two-component fermions at $\kappa = 0$ and two-component bosons at $\kappa = 1$. At coinciding points $x = y$ the commutation relations (2) are fermionic in nature and, therefore, double occupancy, even of particles of opposite spin, is excluded. We will call (1) the anyonic Gaudin-Yang model as it represents the natural generalization to fractional statistics of the fermionic and bosonic models introduced and studied first by Gaudin [43] and Yang [44]. The study of anyonic systems in 1D is now a mature field with important results derived both in single component (like the anyonic Lieb-Liniger model) [45–64] and multicomponent systems [27, 65–70].

We will consider both static and time-dependent external potentials. In the static case we will consider trapping potentials of the type $V(x) = a_\nu |x|^\nu$, $\nu \geq 1$ (the usual harmonic trapping is obtained for $\nu = 2$ and $a_\nu = m\omega_0^2/2$) but our results are also valid in the case of more general trapping potentials or systems with Dirichlet or Neumann boundary conditions in a box of dimension L (in the Dirichlet case the potential can be thought as $V(x) = 0$ for $x \in [0, L]$ and $V(x) = \infty$ for $x \notin [0, L]$). The case without external potential $V(x) = 0$ and periodic boundary conditions was investigated in [26, 27]. In the time-dependent case we will consider potentials which present a sudden change at $t = 0$ resulting in quantum quenches but as we will see our results are valid also in other nonequilibrium scenarios like the quantum Newton's cradle setup [4]. Prototypical examples are the change of the trap's frequency of a harmonic trapping potential

$$V(x, t) = \begin{cases} m\omega_0^2 x^2/2, & t \leq 0, \\ m\omega_1^2 x^2/2, & t > 0, \end{cases} \quad \omega_0 \neq \omega_1, \quad (3)$$

(the free expansion after the release from a trap is a particular case with $\omega_1 = 0$) and the change of the shape of the trap

$$V(x, t) = \begin{cases} a_\nu |x|^\nu, & t \leq 0, \\ a_{\nu'} |x|^{\nu'}, & t > 0, \end{cases} \quad \nu \neq \nu'. \quad (4)$$

In the time-dependent case we have an initial Hamiltonian denoted by H_I and a final Hamiltonian denoted by H_F . In order to compute the time evolution of the correlators we will consider either the equilibrium groundstate or a

thermal state of the initial Hamiltonian H_I but the subsequent evolution will be given by the final Hamiltonian H_F . Of course, in the static case we have $H_I = H_F$.

In order to highlight the differences between the two-component and single component systems we will make frequent comparisons with results for the anyonic Lieb-Liniger (LL) model [45, 47, 49, 50] described by the Hamiltonian

$$H_{LL} = \int dx \frac{\hbar^2}{2m} \partial_x \Psi^\dagger \partial_x \Psi + g \Psi^\dagger \Psi^\dagger \Psi \Psi + (V(x, t) - \mu) \Psi^\dagger \Psi, \quad (5)$$

where now $\Psi^\dagger(x)$ and $\Psi(x)$ are single component anyonic fields satisfying similar commutation relations like (2). For $\kappa = 1$ the Hamiltonian (5) reduces to the usual bosonic LL model while for $\kappa = 0$ it describes free fermions (single component fermions do not “feel” the contact interaction). From now on we will consider $\hbar = k_B = 1$ with k_B the Boltzmann constant.

A. Eigenstates at $t = 0$

While the homogeneous fermionic and bosonic GY models are integrable for any value of the repulsive interaction (the proof of the integrability in the anyonic case is an open problem) the addition of an external potential breaks this integrability with the exception of zero and infinite repulsion. In the impenetrable case, which is the focus of this paper, we will introduce in a constructive fashion a complete set of eigenstates of the initial Hamiltonian which solve the many-body Schrödinger equation, satisfy the hard-core condition and have the proper symmetry when exchanging two particles of the same type.

At $t = 0$ the eigenstates of the initial Hamiltonian for a system of N particles of which M have spin down are given by

$$|\Phi_{N,M}(\mathbf{j}, \boldsymbol{\lambda})\rangle = \int \prod_{k=1}^N dx_k \sum_{\alpha_1, \dots, \alpha_N = \{\uparrow, \downarrow\}}^{[N,M]} \chi_{N,M}^{\alpha_1 \dots \alpha_N}(\mathbf{x}|\mathbf{j}, \boldsymbol{\lambda}) \Psi_{\alpha_N}^\dagger(x_N) \dots \Psi_{\alpha_1}^\dagger(x_1) |0\rangle, \quad (6)$$

where $\mathbf{x} = (x_1, \dots, x_N)$, the $[N, M]$ over the sum sign means that we sum over combinations of α 's such that M of them are spin down and $N - M$ are spin up and $|0\rangle$ is the Fock vacuum satisfying $\Psi_\alpha(x)|0\rangle = \langle 0|\Psi_\alpha^\dagger(x) = 0$ for all α and x . The eigenstates (6) are indexed by two sets of unequal numbers $\mathbf{j} = (j_1, \dots, j_N)$ and $\boldsymbol{\lambda} = (\lambda_1, \dots, \lambda_M)$ (their meaning will be made clear below) and the normalized wavefunctions are $[\boldsymbol{\alpha} = (\alpha_1 \dots \alpha_N)]$

$$\chi_{N,M}^\alpha(\mathbf{x}|\mathbf{j}, \boldsymbol{\lambda}) = \frac{1}{N!N^{M/2}} \left[\sum_{P \in S_N} \theta(x_{P(1)} < \dots < x_{P(N)}) e^{i \frac{\pi \kappa}{2} \sum_{1 \leq a < b \leq N} \text{sign}(x_a - x_b)} \eta_{N,M}^{(\boldsymbol{\alpha}, P\boldsymbol{\alpha})}(\boldsymbol{\lambda}) \right] \det_N [\phi_{j_a}(x_b)], \quad (7)$$

with the sum being taken over all the permutations of N elements denoted by S_N , $\theta(x_1 < \dots < x_N) = \prod_{l=2}^N \theta(x_l - x_{l-1})$ with $\theta(x)$ the Heaviside function and $P\boldsymbol{\alpha} = (\alpha_{P(1)} \dots \alpha_{P(N)})$. In the right hand side of (7) the Slater determinant is constructed from the eigenfunctions of the initial single-particle Hamiltonian defined by

$$H_I^{SP}(x) \phi_j(x) = \varepsilon(j) \phi_j(x), \quad H_I^{SP}(x) = -\frac{1}{2m} \frac{\partial^2}{\partial x^2} + V(x, t \leq 0). \quad (8)$$

For example, if $V(x, t \leq 0) = m\omega_0^2 x^2/2$ then $\phi_j(x)$ is the j -th Hermite function of frequency ω_0 and $\varepsilon(j) = \omega_0(j+1/2)$. The spin sector is described by $\eta_{N,M}^{(\boldsymbol{\alpha}, P\boldsymbol{\alpha})}(\boldsymbol{\lambda})$ which are the wavefunctions of the XX spin-chain on a lattice with N sites and M spins down. Explicitly, we have [71]

$$\eta_{N,M}^{(\boldsymbol{\alpha}, P\boldsymbol{\alpha})}(\boldsymbol{\lambda}) = \prod_{1 \leq a < b \leq M} \text{sign}(n_b - n_a) \det_M [e^{i n_a \lambda_b}], \quad (9)$$

where $\boldsymbol{\lambda} = (\lambda_1, \dots, \lambda_M)$ are solutions of the Bethe ansatz equations for the spin problem

$$e^{i \lambda_a N} = (-1)^{M-1}, \quad a = 1, \dots, M, \quad (10)$$

and $\mathbf{n} = (n_1, \dots, n_M)$ are a set of integers which are the positions of the spin down particles in the set $(\alpha_{P(1)}, \dots, \alpha_{P(N)})$. For example, if $\boldsymbol{\alpha} = (\downarrow \downarrow \uparrow)$ and $P = (3214)$ then the set of n 's for $\boldsymbol{\alpha}$ is $\mathbf{n} = (1, 2)$ while for $P\boldsymbol{\alpha} = (\uparrow \downarrow \downarrow \uparrow)$ we have $\mathbf{n} = (2, 3)$.

The wavefunctions (7) are the natural generalization of the Bethe Ansatz solution for the impenetrable Gaudin-Yang model [26] in the presence of an external potential. They exhibit factorization of the spin and charge degrees of freedom characteristic of impenetrable multicomponent systems [72–80], solve the many-body Schrödinger equation, vanish when two coordinates coincide (hard-core condition), have the appropriate symmetry when exchanging two particles of the same type

$$\chi_{N,M}^{\alpha_1 \dots \alpha_i, \alpha_{i+1} \dots \alpha_N}(x_1, \dots, x_i, x_{i+1}, \dots, x_N) = -e^{i\pi\kappa \text{sign}(x_i - x_{i+1})} \chi_{N,M}^{\alpha_1 \dots \alpha_{i+1}, \alpha_i \dots \alpha_N}(x_1, \dots, x_{i+1}, x_i, \dots, x_N), \quad (11)$$

and form a complete set. We should point out that while we chose for the description of the spin sector the XX spin chain wavefunctions an equally valid alternative, but not as computationally efficient, is represented by the XXX spin chain wavefunctions.

The eigenstates (6) are normalized $\langle \Phi_{N,M}(\mathbf{j}, \boldsymbol{\lambda}) | \Phi_{N',M'}(\mathbf{j}', \boldsymbol{\lambda}') \rangle = \delta_{N,N'} \delta_{M,M'} \delta_{\mathbf{j},\mathbf{j}'} \delta_{\boldsymbol{\lambda},\boldsymbol{\lambda}'}$ and satisfy $H_I |\Phi_{N,M}(\mathbf{j}, \boldsymbol{\lambda})\rangle = E_{N,M}(\mathbf{j}) |\Phi_{N,M}(\mathbf{j}, \boldsymbol{\lambda})\rangle$ with

$$E_{N,M}(\mathbf{j}) = \sum_{l=1}^N (\varepsilon(j_l) - \mu + B) - 2MB, \quad (12)$$

The spectrum of the impenetrable anyonic Gaudin-Yang model is independent on the spin state and statistics resulting in large degeneracies of the groundstate and excited states. At zero temperature even an infinitesimal magnetic field totally polarizes the system which is then equivalent to the LL model.

B. Time evolution of the eigenstates

The time evolution of the eigenstates (6) can be easily determined by taking into account that due to the impenetrability of the particles the spin degrees of freedom are effectively frozen which means that the dynamics is encoded in the charge degrees of freedom (the proof is almost identical with the one presented in [20] for the Bose-Fermi mixture). This means that the time evolved eigenstates are

$$e^{-itH_F} |\Phi_{N,M}(\mathbf{j}, \boldsymbol{\lambda})\rangle = e^{-it[(-\mu+B)N - 2BM]} |\Phi_{N,M}(t|\mathbf{j}, \boldsymbol{\lambda})\rangle, \quad (13)$$

where $|\Phi_{N,M}(t|\mathbf{j}, \boldsymbol{\lambda})\rangle$ is described by (6) with the time dependent wavefunction given by

$$\chi_{N,M}^{\alpha}(\mathbf{x}, t|\mathbf{j}, \boldsymbol{\lambda}) = \frac{1}{N!N^{M/2}} \left[\sum_{P \in S_N} \theta(x_{P(1)} < \dots < x_{P(N)}) e^{i\frac{\pi\kappa}{2} \sum_{1 \leq a < b \leq N} \text{sign}(x_a - x_b)} \eta_{N,M}^{(\alpha, P\alpha)}(\boldsymbol{\lambda}) \right] \det_N [\phi_{j_a}(x_b, t)]. \quad (14)$$

In the time independent case ($H_I = H_F$) the time evolved single particle orbitals appearing in the Slater determinant on the right hand side of (14) are given by

$$\phi_j(x, t) = e^{-i\varepsilon(j)t} \phi_j(x, 0), \quad (15)$$

with $\phi_j(x, 0)$ and $\varepsilon(j)$ the eigenfunctions and eigenenergies of the single particle Hamiltonian (8). In the time dependent case ($H_I \neq H_F$) $\phi_j(x, t)$ is the unique solution of the Schrödinger equation

$$i \frac{\partial \phi_j(x, t)}{\partial t} = H_F^{SP}(x) \phi_j(x, t), \quad H_F^{SP}(x) = -\frac{1}{2m} \frac{\partial^2}{\partial x^2} + V(x, t > 0), \quad (16)$$

satisfying the initial boundary condition $\phi_j(x, 0) = \phi_j(x)$ where $\phi_j(x)$ is an eigenfunction of the initial single particle Hamiltonian (8).

C. Correlators

We are interested in deriving efficient numerical representations for the space-, time-, and temperature-dependent correlation functions of the Gaudin-Yang model for a system prepared in a grandcanonical thermal state of the initial Hamiltonian H_I described by the chemical potential μ , magnetic field B and temperature T . We will investigate two correlators ($\sigma \in \{\uparrow, \downarrow\}$):

$$g_{\sigma}^{(-)}(x, t; y, t') = \langle \Psi_{\sigma}^{\dagger}(x, t) \Psi_{\sigma}(y, t') \rangle_{\mu, B, T},$$

$$\begin{aligned}
&= \text{Tr} \left[e^{-H_I/T} \Psi_\sigma^\dagger(x, t) \Psi_\sigma(y, t') \right] / \text{Tr} \left[e^{-H_I/T} \right], \\
&= \sum_{N=0}^{\infty} \sum_{M=0}^{N+1} \sum_{j_1 < \dots < j_{N+1}} \sum_{\lambda_1 < \dots < \lambda_M} \frac{e^{-E_{N+1, M}(\mathbf{j}, \boldsymbol{\lambda})/T}}{\mathcal{Z}} \langle \Phi_{N+1, M}(\mathbf{j}, \boldsymbol{\lambda}) | \Psi_\sigma^\dagger(x, t) \Phi_\sigma(y, t') | \Phi_{N+1, M}(\mathbf{j}, \boldsymbol{\lambda}) \rangle, \quad (17)
\end{aligned}$$

and

$$\begin{aligned}
g_\sigma^{(+)}(x, t; y, t') &= \langle \Psi_\sigma(x, t) \Psi_\sigma^\dagger(y, t') \rangle_{\mu, B, T}, \\
&= \text{Tr} \left[e^{-H_I/T} \Psi_\sigma(x, t) \Psi_\sigma^\dagger(y, t') \right] / \text{Tr} \left[e^{-H_I/T} \right], \\
&= \sum_{N=0}^{\infty} \sum_{M=0}^N \sum_{q_1 < \dots < q_N} \sum_{\mu_1 < \dots < \mu_M} \frac{e^{-E_{N, M}(\mathbf{q}, \boldsymbol{\mu})/T}}{\mathcal{Z}} \langle \Phi_{N, M}(\mathbf{q}, \boldsymbol{\mu}) | \Psi_\sigma(x, t) \Phi_\sigma^\dagger(y, t') | \Phi_{N, M}(\mathbf{q}, \boldsymbol{\mu}) \rangle, \quad (18)
\end{aligned}$$

where

$$\mathcal{Z} = \text{Tr} \left[e^{-H_I/T} \right] = \sum_{N=0}^{\infty} \sum_{M=0}^N \sum_{q_1 < \dots < q_N} \sum_{\mu_1 < \dots < \mu_M} e^{-E_{N, M}(\mathbf{q}, \boldsymbol{\mu})/T}, \quad (19)$$

is the partition function of the initial Hamiltonian in the grandcanonical ensemble described by μ and B at temperature T . In (17) and (18) the time evolution is dictated by the final Hamiltonian H_F and the evolved operators are given by

$$\Psi_\sigma(x, t) = e^{iH_F t} \Psi_\sigma(x) e^{-iH_F t}, \quad \Psi_\sigma^\dagger(x, t) = e^{iH_F t} \Psi_\sigma^\dagger(x) e^{-iH_F t}. \quad (20)$$

The real space densities $\rho_\sigma(x, t)$ and momentum distribution functions (MDFs) $n_\sigma(k, t)$ can be obtained from the equal-time correlator $g_\sigma^{(-)}(x, t; y, t)$ using

$$\rho_\sigma(x, t) = g_\sigma^{(-)}(x, t; x, t), \quad n_\sigma(k, t) = \frac{1}{2\pi} \int \int e^{-ik(x-y)} g_\sigma^{(-)}(x, t; y, t) dx dy. \quad (21)$$

III. FORM FACTORS

The derivation of the determinant representations for the correlators (17) and (18) is relatively involved requiring several steps. In the first step we are going to compute the form factors which appear in the decomposition of the mean values of bilocal operators present in the definition of the correlators. Then, the form factors can be summed using a method which can be understood as a modification of the Cauchy-Binet formula [21, 23, 26] resulting in a determinant representation for the mean values. In the third step we take the thermodynamic limit and use the von Koch's determinant formula to obtain the desired result. Before we present the derivation we make an important observation. Due to the $SU(2)$ symmetry of the Hamiltonian (1) it is sufficient to study only one type of correlators, the other type can be easily obtained using the relation $g_\uparrow^{(\pm)}(x, t; y, t' | B) = g_\downarrow^{(\pm)}(x, t; y, t' | -B)$.

We will start by computing the form factors. The mean values of bilocal operators appearing in the right hand-side of (17) and (18) can be written as sums over form factors as follows. Using the completeness of the eigenstates $\mathbf{1} = \sum_{N=0}^{\infty} \sum_{M=0}^N \sum_{\substack{q_1 < \dots < q_N \\ \mu_1 < \dots < \mu_M}} |\Phi_{N, M}(\mathbf{q}, \boldsymbol{\mu})\rangle \langle \Phi_{N, M}(\mathbf{q}, \boldsymbol{\mu})|$, we obtain (the bar denotes complex conjugation)

$$\langle \Phi_{N+1, M}(\mathbf{j}, \boldsymbol{\lambda}) | \Psi_\sigma^\dagger(x, t) \Psi_\sigma(y, t') | \Phi_{N+1, M}(\mathbf{j}, \boldsymbol{\lambda}) \rangle = \sum_{\substack{q_1 < \dots < q_N \\ \mu_1 < \dots < \mu_M}} \overline{\mathcal{F}}_{N, M}^{(\sigma)}(\mathbf{j}, \boldsymbol{\lambda}; \mathbf{q}, \boldsymbol{\mu} | x, t) \mathcal{F}_{N, M}^{(\sigma)}(\mathbf{j}, \boldsymbol{\lambda}; \mathbf{q}, \boldsymbol{\mu} | y, t'), \quad (22)$$

and

$$\langle \Phi_{N, \bar{M}}(\mathbf{q}, \boldsymbol{\mu}) | \Psi_\sigma(x, t) \Psi_\sigma^\dagger(y, t') | \Phi_{N, \bar{M}}(\mathbf{q}, \boldsymbol{\mu}) \rangle = \sum_{\substack{j_1 < \dots < j_{N+1} \\ \lambda_1 < \dots < \lambda_M}} \mathcal{F}_{N, M}^{(\sigma)}(\mathbf{j}, \boldsymbol{\lambda}; \mathbf{q}, \boldsymbol{\mu} | x, t) \overline{\mathcal{F}}_{N, M}^{(\sigma)}(\mathbf{j}, \boldsymbol{\lambda}; \mathbf{q}, \boldsymbol{\mu} | y, t'), \quad (23)$$

where

$$\mathcal{F}_{N, M}^{(\sigma)}(\mathbf{j}, \boldsymbol{\lambda}; \mathbf{q}, \boldsymbol{\mu} | x, t) = \langle \Psi_{N, \bar{M}}(\mathbf{q}, \boldsymbol{\mu}) | \Psi_\sigma(x, t) | \Phi_{N+1, M}(\mathbf{j}, \boldsymbol{\lambda}) \rangle, \quad (24)$$

is a general form factor of the $\Psi_\sigma(x, t)$ operator on arbitrary states $(\mathbf{j}, \boldsymbol{\lambda})$ in the $(N + 1, M)$ -sector and $(\mathbf{q}, \boldsymbol{\mu})$ in the (N, \bar{M}) -sector ($|\Phi_{N,-1}(\mathbf{j}, \boldsymbol{\lambda})\rangle = 0$ by convention) and

$$\bar{M} = \begin{cases} M & \text{if } \sigma = \uparrow, \\ M - 1 & \text{if } \sigma = \downarrow. \end{cases} \quad (25)$$

The form factor of the $\Psi_\sigma^\dagger(x, t)$ operator is given by the complex conjugate of (24) i.e., $\bar{\mathcal{F}}_{N,M}^{(\sigma)}(\mathbf{j}, \boldsymbol{\lambda}; \mathbf{q}, \boldsymbol{\mu}|x, t)$. In the following we will not write explicitly the dependence of the form factors on the state parameters when there is no risk of confusion.

The derivation of the determinant representation for the form factors is presented in Appendix A. It reads

$$\mathcal{F}_{N,M}^{(\sigma)}(\mathbf{j}, \boldsymbol{\lambda}; \mathbf{q}, \boldsymbol{\mu}|x, t) = \frac{e^{it\mu_\sigma} e^{-i\frac{\pi\kappa N}{2}}}{N^{\bar{M}/2} (N+1)^{M/2}} (-1)^{\delta_{\sigma,\downarrow}(M-1)} \det_M B_\sigma(\boldsymbol{\lambda}, \boldsymbol{\mu}) \det_{N+1} D(\mathbf{j}, \mathbf{q}|x, t), \quad (26)$$

where $\mu_\uparrow = \mu - B$, $\mu_\downarrow = \mu + B$. This representation is factorized with the charge degrees of freedom being described by $D(\mathbf{j}, \mathbf{q}|x, t)$ a square matrix of dimension $N + 1$ and elements

$$[D(\mathbf{j}, \mathbf{q}|x, t)]_{ab} = \begin{cases} f(j_a, q_b|x, t) & \text{for } a = 1, \dots, N+1; b = 1, \dots, N, \\ \phi_{j_a}(x, t) & \text{for } a = 1, \dots, N+1; b = N+1. \end{cases} \quad (27)$$

with (L_+ is the right boundary of the system)

$$f(j, q|x, t) = \delta_{j,q} - (1 - e^{i\pi\kappa\bar{\omega}\nu}) \int_x^{L_+} \bar{\phi}_q(v, t) \phi_j(v, t) dv. \quad (28)$$

where $\omega = e^{i\Lambda}$, $\nu = e^{i\Theta}$ with $\Lambda = \sum_{a=1}^M \lambda_a$, $\Theta = \sum_{b=1}^{\bar{M}} \mu_b$. The spin degrees of freedom are described by determinants of matrices with dimension M and elements $[B_\uparrow(\boldsymbol{\lambda}, \boldsymbol{\mu})]_{ab} = \sum_{n=1}^N e^{in(\lambda_a - \mu_b)}$, $a, b = 1, \dots, M$ in the spin-up case and

$$[B_\downarrow(\boldsymbol{\lambda}, \boldsymbol{\mu})]_{ab} = \begin{cases} \sum_{n=1}^N e^{in(\lambda_a - \mu_b)} & \text{for } a = 1, \dots, M; b = 1, \dots, M-1, \\ 1 & \text{for } a = 1, \dots, M; b = M, \end{cases} \quad (29)$$

for the spin-down case.

IV. DETERMINANT REPRESENTATIONS FOR THE CORRELATION FUNCTIONS

Using the formulas for the form factors from the previous section the mean values (22) and (23) can be summed obtaining rather cumbersome expressions. The situation becomes simpler in the thermodynamic limit, or, more precisely in the large N limit. The necessary calculations are presented in Appendix B. Before we present our results we need to introduce certain relevant functions and parameters. First we introduce the parameter $\gamma = (1 + e^{2B/T})$ and the building block of our representations the function

$$f(j, q|\eta, x, t) = \delta_{j,q} - \left[1 - e^{i(\pi\kappa - \eta)} \right] \int_x^\infty \bar{\phi}_q(v, t) \phi_j(v, t) dv. \quad (30)$$

We will also need

$$F(\gamma, \eta) = 1 + \sum_{p=1}^\infty \gamma^{-p} (e^{i\eta p} + e^{-i\eta p}), \quad \vartheta(a) = \frac{e^{-B/T}}{2 \cosh(B/T) + e^{(\varepsilon(a) - \mu)/T}}, \quad (31)$$

and we note that $F(\gamma = 1, \eta) = 2\pi\delta(\eta)$ and that $\theta(a)$ can be understood as the Fermi function for the spin up particles of the two-component system (see Appendix C). Now we can state on the main results of our paper. The space-, time-, and temperature-dependent correlation functions of the anyonic GY model in a trapping potential have the following determinant representations:

$$g_\uparrow^{(-)}(x, t; y, t') = \frac{e^{-i(t-t')\mu_\uparrow}}{2\pi} \int_{-\pi}^\pi F(\gamma, \eta) \left[\det \left(1 + \gamma V^{(T,-)}(\eta) + R^{(T,-)} \right) - \det \left(1 + \gamma V^{(T,-)}(\eta) \right) \right] d\eta, \quad (32)$$

with $[V^{(T,-)}]_{ab} = \sqrt{\vartheta(a)}(U_{ab}^{(-)} - \delta_{a,b})\sqrt{\vartheta(b)}$ and $[R^{(T,-)}]_{ab} = \sqrt{\vartheta(a)}R_{ab}^{(-)}\sqrt{\vartheta(b)}$ where $U^{(-)}$ and $R^{(-)}$ are infinite matrices with elements

$$U_{ab}^{(-)}(x, t; y, t' | \eta) = \sum_{q=1}^{\infty} \bar{f}(a, q | \eta, x, t) f(b, q | \eta, y, t'), \quad a, b = 1, \dots, \quad (33a)$$

$$R_{ab}^{(-)}(x, t; y, t') = \bar{\phi}_a(x, t) \phi_b(y, t'), \quad a, b = 1, \dots. \quad (33b)$$

For the second type of correlators the following representation is valid

$$g_{\uparrow}^{(+)}(x, t; y, t') = \frac{e^{i(t-t')\mu_{\uparrow}}}{2\pi} \int_{-\pi}^{\pi} F(\gamma, \eta) \left[\det \left(1 + \gamma V^{(T,+)}(\eta) - \gamma R^{(T,+)}(\eta) \right) + (g-1) \det \left(1 + \gamma V^{(T,+)}(\eta) \right) \right] d\eta, \quad (34)$$

with $[V^{(T,+)}]_{ab} = \sqrt{\vartheta(a)}(U_{ab}^{(+)} - \delta_{a,b})\sqrt{\vartheta(b)}$ and $[R^{(T,+)}]_{ab} = \sqrt{\vartheta(a)}R_{ab}^{(+)}\sqrt{\vartheta(b)}$ where $U^{(+)}$ and $R^{(+)}$ are infinite matrices with elements

$$U_{ab}^{(+)}(x, t; y, t' | \eta) = \sum_{j=1}^{\infty} f(j, b | \eta, x, t) \bar{f}(j, a | \eta, y, t'), \quad a, b = 1, \dots, \quad (35)$$

$$R_{ab}^{(+)}(x, t; y, t' | \eta) = \bar{e}_a(x, t; y, t' | \eta) e_b(x, t; y, t' | \eta), \quad a, b = 1, \dots, \quad (36)$$

$$e_a(x, t; y, t' | \eta) = \sum_{j=1}^{\infty} f(j, a | \eta, x, t) \bar{\phi}_j(y, t'), \quad a = 1, \dots, \quad (37)$$

$$\bar{e}_a(x, t; y, t' | \eta) = \sum_{j=1}^{\infty} \bar{f}(j, a | \eta, y, t') \phi_j(x, t), \quad a = 1, \dots, \quad (38)$$

and

$$g(x, t; y, t') = \sum_{j=1}^{\infty} \phi_j(x, t) \bar{\phi}_j(y, t'). \quad (39)$$

We make an observation. The terms in the square parenthesis of (32) and (32) represent the single component equivalent field-field correlators of LL anyons (see [29, 30]) with statistics parameter $\kappa - \eta/\pi$ and Fermi function defined in (31). A similar proposal was made in [81] in the case of spin- $\frac{1}{2}$ fermions on the lattice. Our results show that the transformation introduced in [81] it is valid also in the continuum case and can be extended for arbitrary statistics.

V. EQUAL-TIME CORRELATORS

In order to study the nonequilibrium dynamics of the GY model in several scenarios of interest, like harmonic trapping with variable frequency or the quantum Newton's cradle setup, it is sufficient to consider the $g_{\uparrow}^{(-)}(x, t; y, t)$ correlator from which the dynamics of the real space densities and momentum distributions can be computed using (21). In the equal-time case $t = t'$ the representation for the $g_{\uparrow}^{(-)}(x, t; y, t) \equiv g_{\uparrow}^{(-)}(x, y | t)$ correlator simplifies considerably. Using the fact that the time evolved eigenfunctions are orthonormal

$$\int_{L_-}^{L_+} \bar{\phi}_q(v, t) \phi_j(v, t) dv = \delta_{j,q}, \quad \sum_{j=1}^{\infty} \bar{\phi}_j(w, t) \phi_j(v, t) = \delta(w-v), \quad (40)$$

in Appendix D we show that in the equal-time case the elements of the $V^{(T,-)}$ matrix simplify to

$$[V^{(T,-)}]_{ab} = - \left(1 - e^{-i \text{sign}(y-x)[\pi\kappa - \eta]} \right) \text{sign}(y-x) \sqrt{\vartheta(a)\vartheta(b)} \int_x^y \bar{\phi}_a(v, t) \phi_b(v, t) dv. \quad (41)$$

The dependence on η is now simple enough that we can integrate in (32). We will denote the difference of determinants appearing in (32) by Ξ . In the case $x \leq y$ we have $\Xi = \sum_{n=0}^{\infty} \gamma^n (e^{-i\pi\kappa} e^{i\eta} - 1)^n A(n)$ where $A(n)$ are coefficients that

do not depend on η . We find

$$\begin{aligned} g_{\uparrow}^{(-)}(x, y|t) &= \int_{-\pi}^{\pi} \frac{d\eta}{2\pi} \left[1 + \sum_{p=1}^{\infty} \gamma^{-p} (e^{i\eta p} + e^{-i\eta p}) \right] \sum_{n=0}^{\infty} \gamma^n (e^{-i\pi\kappa} e^{i\eta} - 1)^n A(n), \\ &= \sum_{n=0}^{\infty} (e^{-i\pi\kappa} - \gamma)^n A(n), \end{aligned} \quad (42)$$

where we have used $(e^{-i\pi\kappa} e^{i\eta} - 1)^n = \sum_{k=0}^n C_k^n (-1)^{n-k} e^{i\eta k} e^{-i\pi\kappa k}$ and $\int_{-\pi}^{\pi} e^{i\eta k} e^{-i\eta p} / (2\pi) = \delta_{k,p}$. In the $y < x$ case we obtain $g_{\uparrow}^{(-)}(x, t; y, t) = \sum_{n=0}^{\infty} (\gamma - e^{i\pi\kappa})^n A(n)$. This means that in the equal-time case the following representation is valid

$$g_{\uparrow}^{(-)}(x, y|t) = \det \left(1 + v^{(T,-)} + r^{(T,-)} \right) - \det \left(1 + v^{(T,-)} \right), \quad (43)$$

with

$$[v^{(T,-)}]_{ab} = - \left[\gamma - e^{-i\pi\kappa \text{sign}(y-x)} \right] \text{sign}(y-x) \sqrt{\vartheta(a)\vartheta(b)} \int_x^y \bar{\phi}_a(v, t) \phi_b(v, t) dv, \quad (44a)$$

$$[r^{(T,-)}]_{ab} = \sqrt{\vartheta(a)} \bar{\phi}_a(x, t) \phi_b(y, t) \sqrt{\vartheta(b)}. \quad (44b)$$

At zero magnetic field and zero temperature the parameter $\gamma = 2$ and $\vartheta(a) = \frac{1}{2}\theta(\mu - \varepsilon(a))$. The infinite matrices appearing in (44) are replaced with finite matrices of dimension N with N being the number of energy levels smaller than μ and elements

$$[v^{(0,-)}]_{ab} = -\frac{1}{2} \left(2 - e^{-i\pi\kappa \text{sign}(y-x)} \right) \text{sign}(y-x) \int_x^y \bar{\phi}_a(v, t) \phi_b(v, t) dv, \quad a, b = 1, \dots, N, \quad (45a)$$

$$[r^{(0,-)}]_{ab} = \frac{1}{2} \bar{\phi}_a(x, t) \phi_b(y, t), \quad a, b = 1, \dots, N. \quad (45b)$$

We make an important observation. The zero temperature determinant representation (43) with matrices (45) describes the correlators in the spin-incoherent regime [25, 82–88] which is obtained by taking first the limit of infinite repulsion and then $T \rightarrow 0$. Finding a determinant representation for the impenetrable GY model in the Tomonaga-Luttinger regime, which is obtained by taking first the limit $T \rightarrow 0$ and then the limit of infinite repulsion, is an open problem [83, 85].

We should point out that the representation (43) is extremely efficient from the numerical point of view (the main computational effort comes from the evaluation of the partial overlaps) allowing for the exact investigation of systems with hundreds of particles at zero temperature and tens of particles at very high temperatures, which is more than enough for comparison with current experiments (see, for example, the recent experiment [42] where $N = 32$ atoms per tube at zero temperature). Similar representations for single component systems in the continuum can be found in [35–38].

VI. LENARD'S FORMULA

In Ref. [22] Lenard used the Bose-Fermi mapping to derive an expansion of single component bosonic correlators in terms of free fermionic correlators which was independent on the statistical ensemble and interparticle potential as long as the hard-core condition was satisfied. In Appendix E we show that the determinant representation (43) for the equal-time correlators is equivalent to the following multicomponent generalization of Lenard's formula:

$$g_{\uparrow}^{(-)}(x, y|t) = g_{\uparrow}^{FF}(x, y|t) + \sum_{j=1}^{\infty} \frac{(-\xi)^j}{j!} \int_x^y dx_1 \cdots \int_x^y dx_j g_{\uparrow}^{FF} \left(\begin{matrix} x & x_1 & \cdots & x_j \\ y & x_1 & \cdots & x_j \end{matrix}; t \right), \quad (46)$$

with

$$\xi = \left[\gamma - e^{-i\pi\kappa \text{sign}(y-x)} \right] \text{sign}(y-x), \quad (47)$$

and $g_{\uparrow}^{FF}(x, y|t) = \sum_{a=1}^{\infty} \vartheta(a) \bar{\phi}_a(x, t) \phi_a(y, t)$ which can be understood as the field-field correlation function of a system of free fermions with Fermi function $\vartheta(a)$ defined in (31). In (46) we have used the notation

$$g_{\uparrow}^{FF} \left(\begin{array}{cccc} x & x_1 & \cdots & x_j \\ y & x_1 & \cdots & x_j \end{array}; t \right) = \begin{vmatrix} g_{\uparrow}^{FF}(x, y|t) & g_{\uparrow}^{FF}(x, x_1|t) & \cdots & g_{\uparrow}^{FF}(x, x_j|t) \\ g_{\uparrow}^{FF}(x_1, y|t) & g_{\uparrow}^{FF}(x_1, x_1|t) & \cdots & g_{\uparrow}^{FF}(x_1, x_j|t) \\ \vdots & \vdots & \ddots & \vdots \\ g_{\uparrow}^{FF}(x_j, y|t) & g_{\uparrow}^{FF}(x_j, x_1|t) & \cdots & g_{\uparrow}^{FF}(x_j, x_j|t) \end{vmatrix}. \quad (48)$$

The correlator $g_{\downarrow}(x, y|t)$ has a similar representation as (46) with B replaced by $-B$ in the expressions for γ and the Fermi function $\vartheta(a)$.

At zero temperature and zero magnetic field we have $g_{\uparrow}^{FF}(x, y|t) = \frac{1}{2} \sum_{a=1}^N \bar{\phi}_a(x, t) \phi_a(y, t)$ where N is the number of particles for the balanced system in the ground state. The generalization of Lenard's formula for the balanced system takes the form $[g_{\uparrow}^{(-)}(x, y|t) = g_{\downarrow}^{(-)}(x, y|t)]$

$$g_{\uparrow}^{(-)}(x, y|t) = \frac{1}{2} \left[g_{\uparrow}^{FF,0}(x, y|t) + \sum_{j=1}^{\infty} \frac{(-\xi_0)^j}{j!} \int_x^y dx_1 \cdots \int_x^y dx_j g_{\uparrow}^{FF,0} \left(\begin{array}{cccc} x & x_1 & \cdots & x_j \\ y & x_1 & \cdots & x_j \end{array}; t \right) \right], \quad (49)$$

with

$$\xi_0 = \frac{1}{2} \left[2 - e^{-i\pi\kappa \text{sign}(y-x)} \right] \text{sign}(y-x), \quad g_{\uparrow}^{FF,0}(x, y|t) = \sum_{a=1}^N \bar{\phi}_a(x, t) \phi_a(y, t). \quad (50)$$

Lenard's formula (46) is extremely useful in deriving short distance expansions for the correlators, from which the Tan contacts which govern the $C(t)/k^4$ tails of the momentum distributions can be extracted, but it can also be used to obtain Painlevé transcendent representations for finite size systems in equilibrium at zero temperature. Let us show how this can be done. The main observation is that (49) can be understood as the first Fredholm minor of the Fredholm integral operator $1 - \xi_0 \hat{g}_{\uparrow}^{FF,0}$ acting on $[x, y]$ and with kernel $g_{\uparrow}^{FF,0}(\lambda, \mu)$. Using Hurwitz formula [89] we find

$$g_{\uparrow}^{(-)}(x, y) = \frac{1}{2} R_{\uparrow}^{FF}(x, y) \det \left(1 - \xi_0 \hat{g}_{\uparrow}^{FF,0} \right), \quad (51)$$

with the resolvent satisfying the integral equation

$$R_{\uparrow}^{FF}(\lambda, \mu) = g_{\uparrow}^{FF,0}(\lambda, \mu) + \xi_0 \int_x^y g_{\uparrow}^{FF,0}(\lambda, \nu) R_{\uparrow}^{FF}(\nu, \mu) d\nu. \quad (52)$$

In the particular case at when x and y are chosen such that they are symmetrical about the origin, say $[-x, x]$, and using $\frac{d}{dx} \log \det \left(1 - \xi_0 \hat{g}_{\uparrow}^{FF} \right) = -2R_{\uparrow}^{FF}(x, x)$ we obtain

$$g_{\uparrow}^{(-)}(-x, x) = \frac{1}{2} R_{\uparrow}^{FF}(-x, x) \exp \left(-2 \int_0^x R_{\uparrow}^{FF}(t, t) dt \right). \quad (53)$$

The importance of the previous formula resides in the fact that the quantities $R_{\uparrow}^{FF}(-x, x)$ and $R_{\uparrow}^{FF}(t, t)$ have previously been calculated in terms of Painlevé transcendents as part of studies on gap probabilities for certain random matrix ensembles [90, 91]. In the harmonic trapping case the relevant ensemble is the Gaussian Unitary Ensemble and the Painlevé transcendent representation can be found in Proposition 5 of [39] with the parameter $\xi = (1 - e^{-i\pi\kappa}/2)$. It is interesting to note that modulo a 1/2 factor the correlators of the finite GY model with harmonic trapping can be expressed in terms of the same P_V transcendent as the single component bosonic system, the only difference being in the boundary conditions. In the case of Dirichlet and Neumann boundary conditions the ensemble of interest is the Jacobi Unitary Ensemble with $a = b = \pm 1/2$ and the transcendent representation can be found in Proposition 6 of [39].

VII. DYNAMICS IN THE CASE OF VARIABLE FREQUENCY

Using the results of Sec. V we can investigate the dynamics of the real space densities and momentum distribution functions of the Gaudin-Yang model in the experimentally relevant case of a trapping potential with variable frequency.

We will focus on the case of free expansion of the gas and the breathing oscillations initiated by a sudden change in the trap's frequency.

In the case of a harmonic potential with variable frequency $V(x, t) = m\omega^2(t)x^2/2$ with $\omega(t \leq 0) = \omega_0$ the single particle eigenfunctions at $t = 0$ are the Hermite functions of frequency ω_0

$$\phi_j(x) = \frac{1}{\sqrt{2^j j!}} \left(\frac{m\omega_0}{\pi} \right)^{1/4} e^{-\frac{m\omega_0^2 x^2}{2}} H_j(\sqrt{m\omega_0}x), \quad (54)$$

where $H_j(x)$ are the Hermite polynomials. The time evolution of the single particle orbitals is given by the scaling transformation ([92], Chap. VII of [93]):

$$\phi_j(x, t) = \frac{1}{\sqrt{b(t)}} \phi_j \left(\frac{x}{b(t)}, 0 \right) \exp \left[i \frac{mx^2}{2} \frac{\dot{b}}{b} - i\varepsilon(j)\tau(t) \right], \quad (55)$$

with $b(t)$ the solution of the Ermakov-Pinney equation $\ddot{b} + \omega^2(t)b = \omega_0^2/b^3$ and initial boundary conditions $b(0) = 1$, $\dot{b}(0) = 0$, $\varepsilon(j) = \omega_0(j + 1/2)$ and $\tau(t) = \int_0^t dt'/b^2(t')$. Due to the fact that the dynamics is encoded only in the charge degrees of freedom the time evolution of the correlators is given by [18–20]

$$g_\sigma^{(-)}(x, y|t) = \frac{1}{b(t)} g_\sigma^{(-)} \left(\frac{x}{b(t)}, \frac{y}{b(t)} \middle| 0 \right) e^{-\frac{i}{b} \frac{\dot{b}}{\omega_0} \frac{x^2 - y^2}{2l_o^2}}, \quad (56)$$

with $l_o = \sqrt{1/m\omega_0}$ the harmonic oscillator length. The time evolution of the densities is

$$\rho_\sigma(x, t) = \frac{1}{b(t)} \rho_\sigma \left(\frac{x}{b(t)} \middle| 0 \right), \quad (57)$$

and in the case of the momentum distributions we have

$$n_\sigma(k, t) = \frac{b}{2\pi} \int \int dx dy g_\sigma^{(-)}(x, y|0) \exp \left[-ib \left(\frac{\dot{b}}{\omega_0} \frac{x^2 - y^2}{2l_o^2} + k(x - y) \right) \right]. \quad (58)$$

These results show that in order to study the exact dynamics in the case of a system with variable frequency it is sufficient to compute the correlators at $t = 0$ and then use Eqs. (56) and (58).

A. Free expansion

Free expansion is described by $\omega(t \leq 0) = \omega_0$ and $\omega(t \geq 0) = 0$ and is ubiquitous in cold gases experiments allowing for the investigation of the MDF. In this case the solution of the Ermakov-Pinney equation is $b(t) = (1 + \omega_0^2 t^2)^{1/2}$. We will consider first the case of balanced systems at zero temperature (note that even an infinitesimal magnetic field will polarize the system at $T = 0$ reducing its study to the single component case). Employing the stationary phase approximation in (58) analytical results on the total asymptotic momentum distribution can be obtained showing that it is the same as the MDF of a system of free fermions in the initial trap. This phenomenon is called dynamical fermionization [36, 94–100] and in the case of the single component bosonic TG gas was experimentally observed in [101]. In the case of bosonic and fermionic spinor gases with any number of components at zero temperature dynamical fermionization of the total momentum distribution was derived by an Alam *et. al* in [18]. For the anyonic GY model using the explicit form of the wavefunctions (7) and the method of [20] it can be shown that the asymptotic momentum distributions are given by

$$n_\sigma(k, t \rightarrow \infty) \sim \frac{1}{2} n_{FF}(k), \quad n(k, t \rightarrow \infty) \sim n_{FF}(k), \quad (59)$$

where $n(k, t) = n_\uparrow(k, t) + n_\downarrow(k, t)$ is the total MDF of the GY model and $n_{FF}(k)$ is the MDF of a similar number of free fermions N in the original trap [$\phi_j(x)$ are defined in (54)]

$$n_{FF}(k) = \frac{1}{2\pi} \int \int e^{-ik(x-y)} g_{FF}^{(-)}(x, y) dx dy, \quad g_{FF}^{(-)}(x, y) = \sum_{i=0}^{N-1} \bar{\phi}_i(x) \phi_i(y). \quad (60)$$

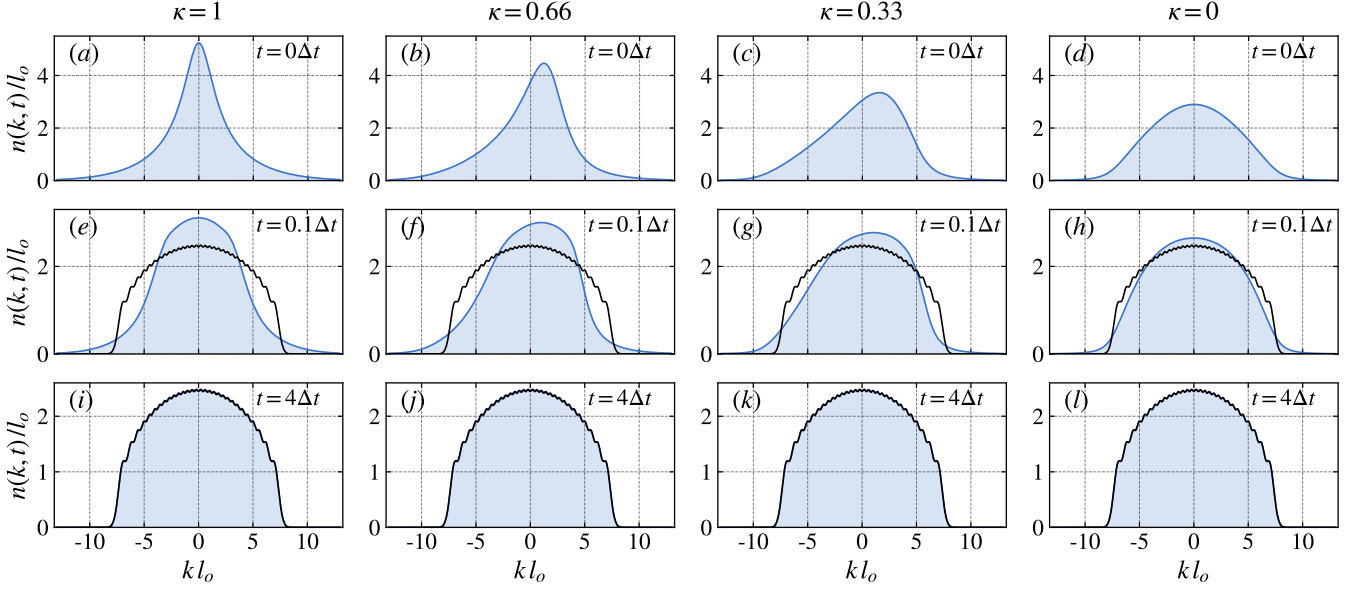


FIG. 1. Momentum distribution functions before (first row) and after free expansion at $t = 0.1\Delta t$ (second row) and $t = 4\Delta t$ (third row) computed using Eqs. (43), (45) and (58). We consider balanced systems of $N = 30$ particles at zero temperature ($\omega_0 = 1, l_o = 1, \Delta t = \pi/\omega_0$) and statistics parameter $\kappa = \{1, 0.66, 0.33, 0\}$. In the second and third row the black line represents the momentum distribution function of a system of free fermions with the same number of particles in the initial harmonic trap Eq. (60).

In Fig. 1 we present the dynamics of the total MDF for a zero temperature balanced anyonic GY model with $N = 30$ particles for different values of the statistical parameter $\kappa = \{1, 0.66, 0.33, 0\}$ and three values of t : before the release from the trap $t = 0$ (first row), immediately after release $t = 0.1\pi/\omega_0$ (second row) and in the asymptotic region $t = 4\pi/\omega_0$ (third row). At $t = 0$ the MDF for the bosonic system ($\kappa = 1$) presents a visible peak at $k = 0$ similar with the one for single component bosons but less pronounced due to the spin-incoherent nature of the system. The fermionic MDF ($\kappa = 0$) of the GY model is also smoothed out compared with the free fermionic MDF which in the presence of the trapping potential presents a number of local maxima equal to the number of particles in the system. The main feature of the MDF for anyonic systems ($\kappa = \{0.66, 0.33\}$) is the asymmetry which is caused by the broken space invariance of the commutation relations (2) resulting in $g_{\sigma}^{(-)}(x, y) = g_{\sigma}^{(-)}(y, x)$ [for the bosonic and fermionic systems $g_{\sigma}^{(-)}(x, y)$ is real and we have $g_{\sigma}^{(-)}(x, y) = g_{\sigma}^{(-)}(y, x)$]. For all systems at large times after the release from the trap the asymptotic momentum distribution approaches the symmetric MDF for free fermions in the initial trap (60) as it can be seen in the last row of Fig. 1.

At finite temperature the situation is more complex. In [20] it was shown that for a trapped system initially found in a thermal state described by the chemical potential μ , magnetic field B and temperature T the asymptotic momentum distribution is the same as the one for spinless free fermions in the initial trap at the same temperature but renormalized chemical potential

$$\mu' = \mu + T \ln[2 \cosh(B/T)]. \quad (61)$$

Explicitly, the asymptotic MDF for each component reads

$$n_{\downarrow}(k, t \rightarrow \infty) \sim \frac{e^{B/T}}{2 \cosh(B/T)} n_{FF}^{\mu'}(k), \quad n_{\uparrow}(k, t \rightarrow \infty) \sim \frac{e^{-B/T}}{2 \cosh(B/T)} n_{FF}^{\mu'}(k), \quad (62)$$

and $n(k, t \rightarrow \infty) \equiv n_{\downarrow}(k, t \rightarrow \infty) + n_{\uparrow}(k, t \rightarrow \infty) = n_{FF}^{\mu'}(k)$ where $n_{FF}^{\mu'}(k)$ is the MDF of trapped spinless free fermions given by

$$n_{FF}^{\mu'}(k) = \frac{1}{2\pi} \int \int e^{-ik(x-y)} g_{FF, \mu'}^{(-)}(x, y) dx dy, \quad g_{FF, \mu'}^{(-)}(x, y) = \sum_{i=0}^{\infty} \frac{1}{1 + e^{(\varepsilon(i) - \mu')/T}} \bar{\phi}_i(x) \phi_i(y). \quad (63)$$

In Fig. 2 we present the time evolution of the MDF after release from the trap for an unbalanced system of $N = 30$

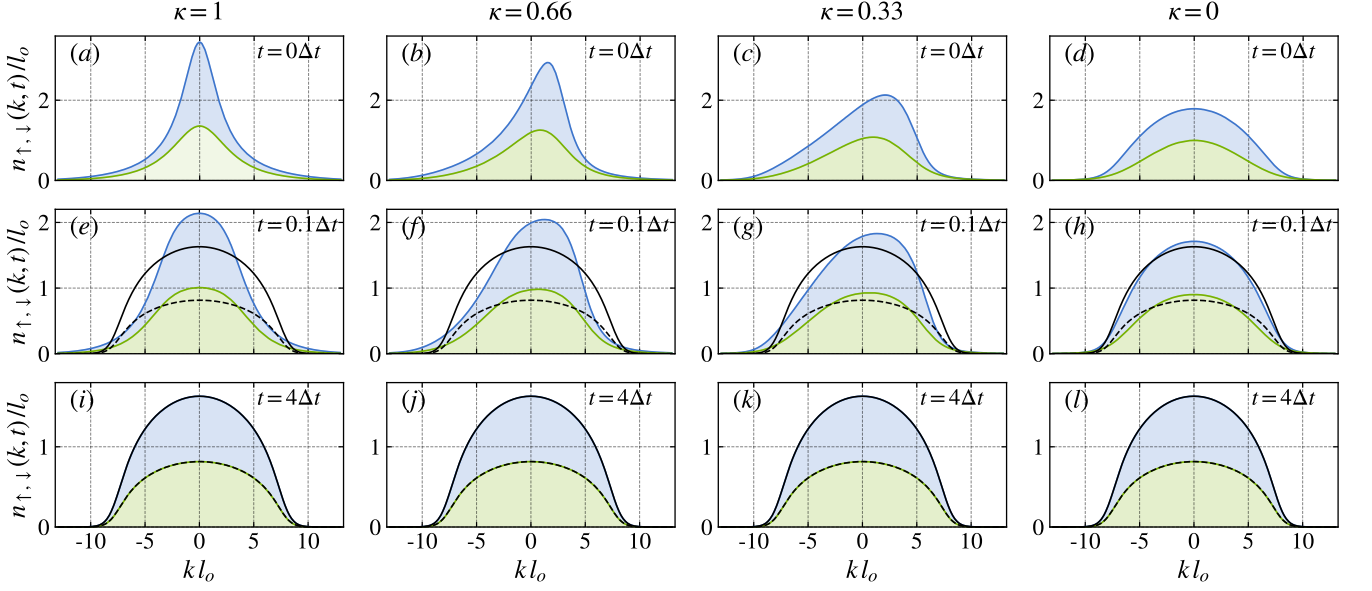


FIG. 2. Momentum distribution functions of an imbalanced system at finite temperature before (first row) and after free expansion at $t = 0.1\Delta t$ (second row) and $t = 4\Delta t$ (third row) computed using Eqs. (43), (44) and (58). Here we consider systems with $N = 30$ particles ($N_{\downarrow} = 20$, $N_{\uparrow} = 10$) at temperature $T = 4$ ($\omega_0 = 1$, $l_o = 1$, $\Delta t = \pi/\omega_0$) and statistics parameter $\kappa = \{1, 0.66, 0.33, 0\}$. The blue (green) continuous lines represent the MDFs of the spin-down (up) particles and in the second and third row the black continuous (dashed) lines represent the analytical result Eq. (62) for the spin-down (up) particles.

particles ($N_{\downarrow} = 20$, $N_{\uparrow} = 10$) at temperature $T = 4$ which shows the perfect agreement with our analytical predictions for the asymptotic distributions (62).

B. Breathing oscillations and collective many-body bounce effect

A confinement quench in which the trap frequency is suddenly changed to a new value initiates breathing oscillations which can be experimentally observed [101, 102]. We will denote the pre-quench frequency by $\omega(t \leq 0) = \omega_0$ and the post-quench frequency by $\omega(t \geq 0) = \omega_1$. In this case the solution of the Ermakov-Pinney equation is given by $b(t) = (1 + \epsilon_0 \sin^2(\omega_1 t))^{1/2}$ with $\epsilon_0 = (\omega_0/\omega_1)^2 - 1$ and describes oscillations between 1 and ω_0/ω_1 with period π/ω_1 .

In Fig. 3 we present and compare the dynamics of the densities and MDFs for a balanced GY model with $N = 30$ particles at zero temperature and the LL model with the same number of particles subjected to a strong confinement quench $\omega_1 = 6\omega_0$. The time evolution of the real space densities, which are the same for both models, is described by self-similar breathing cycles $\rho(x, t) = \rho(x/b(t)|0)/b(t)$ which can be seen in Fig. 3a) and Fig. 3e). The situation is more complex in the case of the MDFs. From Fig. 3b)-d) we see that for the GY model and all values of the statistics parameter the MDF dynamics is no longer self-similar and presents two instances of narrowing: at $\omega_1 t = \pi l$, $l = 0, 1, \dots$ (called outer turning points [40]) when the real density is the broadest and at $\omega_1 t = \frac{\pi}{2} l$, $l = 1, 2, \dots$ (called inner turning points) when the gas is maximally compressed. The additional narrowing at the inner turning point is a manifestation of a many-body collective effect not present in noninteracting systems (see Fig. 3h) which can be understood as a self-reflection of the cloud due to the repulsive interactions. In the case of single component bosons this collective effect was discovered and investigated in [40] and in the case of single component anyonic systems in [38]. The amplitude of the narrowing at the inner turning points depends on statistics being the largest for bosons ($\kappa = 1$) and smallest for fermions ($\kappa = 0$). This can be seen in the evolution of the Full Width at Half Maximum of the MDF presented in Fig. 3j)-l) and can also be explained in terms of the repulsive interactions between the particles: in the bosonic case we have inter and intra-particles interaction while in the fermionic case only particles with opposite pseudo-spins interact with the anyonic case being in between. We will denote $FWHM_{GY}(FWHM_{LL})$ the widths of the relevant quantities for the GY (LL) model. The width differences $\Delta FWHM = FWHM_{GY} - FWHM_{LL}$ plotted in the fourth row of Fig. 3 show that during the time evolution the largest differences in the MDFs of single and two-component systems occur in the vicinities of the inner and outer turning points. For the bosonic and anyonic system with $\kappa = 0.5$ $\Delta FWHM$ is always positive signalling a broader MDF for the two-component system which is

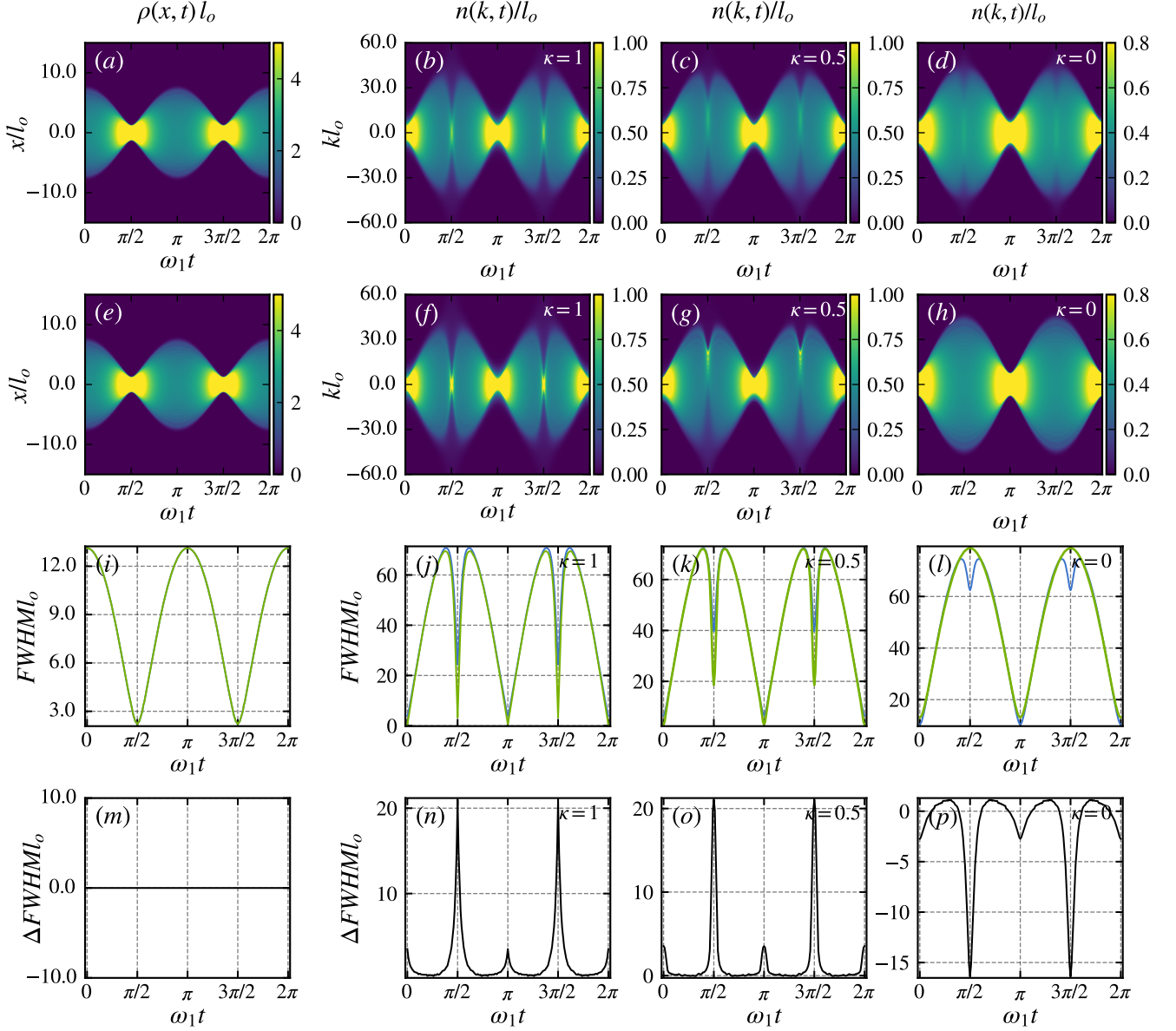


FIG. 3. Breathing oscillations dynamics in the GY and LL models. First row: a) Time dependence of the total density $\rho(x, t)$ (Eq. (57)) and total momentum distribution $n(k, t)$ (Eq. (60)) for $\kappa = 1$ b), $\kappa = 0.5$ c) and $\kappa = 0$ d) in the balanced GY model at zero temperature with $N = 30$ particles after a strong quench of the trap frequency ($\omega_0 = 1, \omega_1 = 6\omega_0, \epsilon_0 \sim -0.972, l_o = 1$). The correlator at $t = 0$ is computed with Eqs. (43) and (45). Second row: e)-h) Same quantities as above for the single component LL model with the same number of particles. Third row: a) Width (FWHM) of the densities [blue (green) line for the GY (LL) model] and momentum distributions j)-l). Fourth row: Width difference $\Delta FWHM = FWHM_{GY} - FWHM_{LL}$ for the densities m) and momentum distributions n)-p).

due to the spin-incoherence of the system (see the discussion in Sec. VIII). In the fermionic case in the vicinities of the inner and outer turning points the MDF of free fermions is wider than the one for the GY model while in between the inner and outer turning points the opposite is true.

VIII. DYNAMICS IN THE NEWTON'S QUANTUM CRADLE SETUP

In the original Quantum Newton Cradle (QNC) experiment [4] a quasi-1D ultracold gas of LL bosons in a weakly harmonic trap is subjected to a sequence of Bragg pulses which splits the initial quasicondensate into two counter-

propagating clouds with momenta centered around $\pm q$. The fact that these clouds undergo repeated oscillations without thermalization like an ordinary gas highlighted the importance of the large number of conservation laws in the description of nonequilibrium 1D quantum systems. From the theoretical point of view the dynamics of single component bosons in the QNC setup has been investigated in [37, 97, 103, 106, 107]. Here, we focus on the two-component Gaudin-Yang model (see also [17] for a GHD approach).

First, let us show how our formalism developed in the previous sections can be applied in the QNC setup. Generalizing the results of [103] in the case of two-component systems we model a Bragg pulse in the Raman-Nath limit [104, 105], in which the motion of the particles during the pulse is neglected, with the Bragg pulse operator

$$U_B(q, A) = e^{-iA \int dx \cos(qx) (\Psi_\uparrow^\dagger(x) \Psi_\uparrow(x) + \Psi_\downarrow^\dagger(x) \Psi_\downarrow(x))}. \quad (64)$$

The action of such an instantaneous pulse on an arbitrary eigenstate of the Hamiltonian (1) is given by

$$|\Phi_{N,M}^{q,A}(\mathbf{j}, \boldsymbol{\lambda})\rangle = U_B(q, A) |\Phi_{N,M}(\mathbf{j}, \boldsymbol{\lambda})\rangle, \quad (65)$$

with $|\Phi_{N,M}^{q,A}(\mathbf{j}, \boldsymbol{\lambda})\rangle$ given by (6) with the wavefunction multiplied by $e^{-iA \sum_{k=1}^N \cos(qx_k)}$. This means that the effect of the Bragg pulse is that in the Slater determinant describing the charge degrees of freedom we have to replace $\phi_j(x)$ with $\phi_j(x) e^{-iA \cos(qx)}$. After the pulse the time evolution is given by the Hamiltonian (1) with $V(x) = m\omega^2 x^2/2$ and the dynamics of the single particle eigenfunctions can be computed analytically using the propagator of the quantum harmonic oscillator

$$K(x, u|t) = \left(\frac{m\omega}{2\pi i \sin(\omega t)} \right)^{1/2} \exp \left(\frac{-m\omega(x^2 + u^2) \cos(\omega t) + 2m\omega x u}{2i \sin(\omega t)} \right), \quad (66)$$

and $\phi_j(x, t) = \int_{-\infty}^{+\infty} K(x, u|t) e^{-iA \cos(qx)} \phi_j(u) du$. One obtains [103]

$$\phi_j(x, t) = \sum_{n=-\infty}^{\infty} I_n(-iA) e^{-in q \cos(\omega t) (x + n q \frac{\sin(\omega t)}{2m\omega})} \phi_j \left(x + n q \frac{\sin(\omega t)}{m\omega} \right) e^{-i\omega(j + \frac{1}{2})t}, \quad (67)$$

with $I_n(x) = \int_0^\pi e^{x \cos \theta} \cos(n\theta) d\theta / \pi$ the modified Bessel function of the first kind. Therefore, the dynamics of the GY model in the quantum Newton's cradle is given by the determinant representation (43) with matrices (44) at finite temperature and (45) at zero temperature with the time-evolved single particle orbitals defined in (67). In the TG regime the time evolution of the GY model in the QNC setup is periodic with period π/ω . This statement can be proved using the relation $I_n(-iA) = I_{-n}(iA)$ (see the integral representation) in (67) resulting in $\phi_j(x, t + \pi/\omega) = e^{-i(j+1/2)\pi} \phi_j(x, t)$. The correlators involve products of wavefunctions of the type $\bar{\chi}_{N,M} \chi_{N,M}$ resulting in cancellation of the phases and therefore the densities and momentum distributions are periodic with period π/ω . In the single component case Berg *et al.* [103] showed that there are two separate time scales in the problem: rapid and trap-insensitive dephasing after the pulse followed by the slow periodic behaviour. The fastest time scale is associated with hydrodynamization and was experimentally observed in single component TG bosons [42]. Below we will investigate the hydrodynamization in the GY model and highlight the differences between the single and two-component case.

Hydrodynamization occurs in systems which are quenched with energies much larger than the ground-state energy and is characterized by a rapid onset of hydrodynamics before local thermal equilibrium is established [41]. Hydrodynamization takes place on the fastest available timescale which is related to the Bragg peak energies and can be seen in the redistribution of energy among distant momentum modes [42]. For Bragg pulses with $A \sim 1$ the hydrodynamization frequency ω_{hd} can be obtained from the difference of the $n = 0$ and $n = \pm 1$ Bragg orders $\omega_{hd} = q^2/2m$ and the associated timescale of hydrodynamization is given by $T_{hd} = 2\pi/\omega_{hd}$.

In order to investigate the action of the Bragg pulse on the MDF and the subsequent time evolution it is useful to remind the reader some analytical results on the correlators of TG gases. For any interaction and geometry the following relation is valid $[\Phi \equiv \Phi_{N,M}(\mathbf{j}, \boldsymbol{\lambda})]$

$$\langle \Phi | U_B^\dagger(q, A) \Psi_\sigma^\dagger(x) \Psi_\sigma(y) U_B(q, A) | \Phi \rangle = e^{-2iA \sin(q \frac{x-y}{2}) \sin(q \frac{x+y}{2})} \langle \Phi | \Psi_\sigma^\dagger(x) \Psi_\sigma(y) | \Phi \rangle \quad (68)$$

which can be proved by using the explicit expression of the mean value on terms of the wavefunctions and the fact that the action of the Bragg operator multiplies the wavefunction of an arbitrary state with $e^{-iA \sum_{k=1}^N \cos(qx_k)}$. Then, performing similar calculations like in the Supplemental Material of [103], one can show that in the case of circular geometry the momentum distribution function after the pulse is given by

$$n_\sigma(k, t = 0) = \sum_{l=-\infty}^{\infty} c_l(A) n_\sigma^{(0)}(k + lq), \quad (69)$$

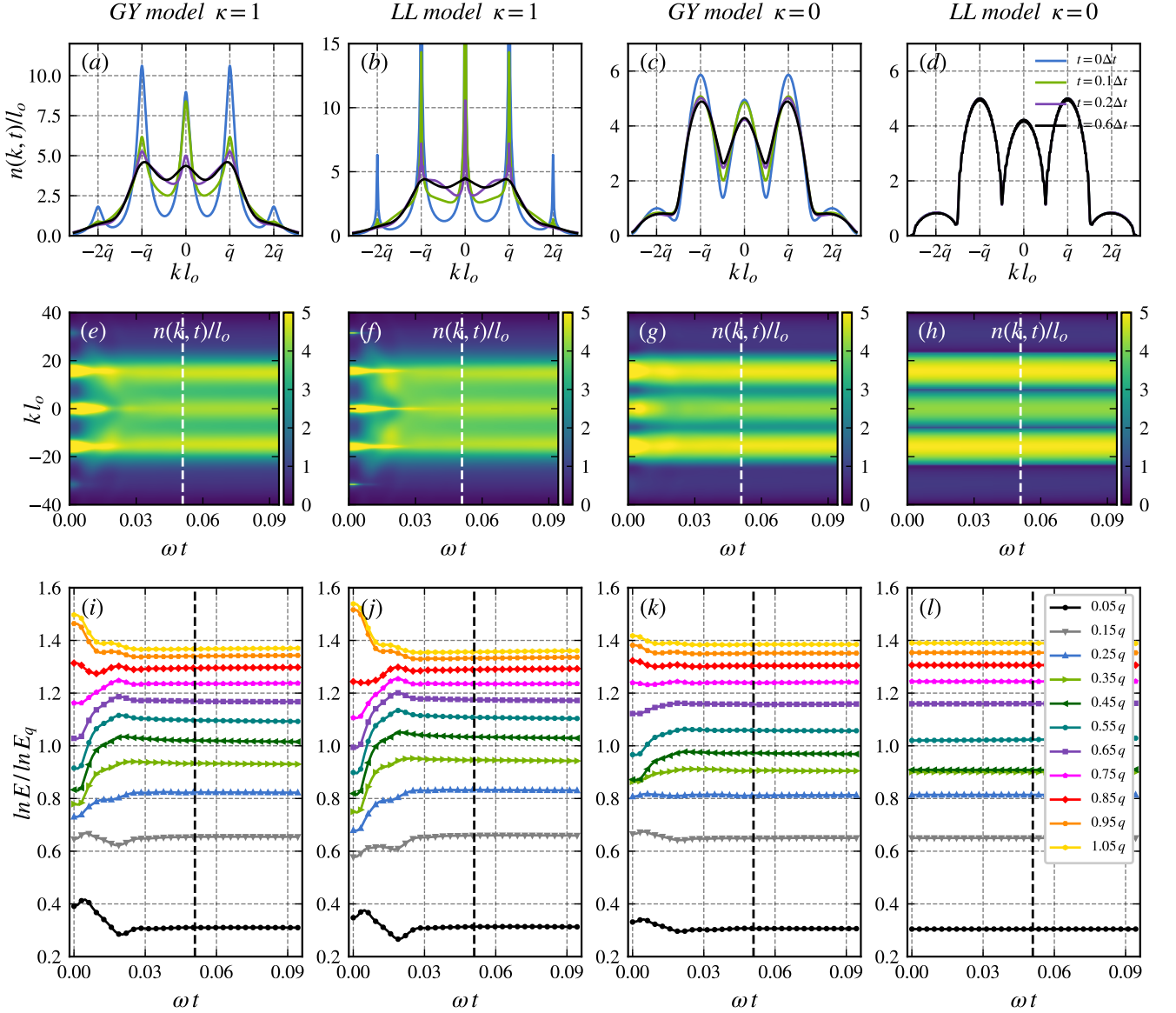


FIG. 4. First row: The momentum distribution functions after the Bragg pulse at $t = \{0, 0.1\Delta t, 0.2\Delta t, 0.6\Delta t\}$ ($\Delta t = \pi/40\omega$) for systems of $N = 32$ particles at zero temperature ($\omega = 1$, $A = 1.5$, $q = 5\pi$, $l_o = 1$, $\bar{q} = ql_o$). We present results for the bosonic GY model a), bosonic LL model b), fermionic GY model c) and single component free fermions (anyonic LL model at $\kappa = 0$) d). The results for the GY model were computed using Eqs. (43), (45) and (67). Second row: Time evolution of the momentum distribution functions showing the rapid population of the modes between the $\pm q$ satellites due to hydrodynamization which is essentially complete by $T_{hd} = 2\pi/\omega_{hd}$ (marked by the white dashed line). Third row: Time evolution of the integrated energy (in units of $E_q = q^2/2m$) in $0.1q$ wide momentum groups. The average momentum of each groups is shown in the legend. The dashed black line marks T_{hd} .

where $n_\sigma^{(0)}(k)$ is the MDF before the pulse and the coefficients $c_l(A)$ depend on the value of A . Eq. (69) shows that in the case of a homogeneous system the MDF after the pulse is a sum of copies of the ground-state MDF at $T = 0$ (thermal MDF at finite temperature) centered around multiples of q . Using the Local Density Approximation one expects that a similar picture holds in the case of weak harmonic trapping. Therefore, it is useful to study the MDF of homogeneous systems. In the case of single component anyons without trapping the large distance asymptotics of the field-field correlators is given by [27, 51, 52]

$$g^{(-)}(x, 0) \equiv \langle \Psi^\dagger(x) \Psi(0) \rangle \sim a \frac{e^{ik_F(\kappa-1)x}}{x^{1-\kappa+\frac{\kappa^2}{2}}} + b \frac{e^{ik_F(\kappa+1)x}}{x^{1+\kappa+\frac{\kappa^2}{2}}}, \quad x > 0, \quad (70)$$

with a, b constants that can be found in [27]. Note that $g^{(-)}(-x, 0) = \overline{g^{(-)}(x, 0)}$. We focus on the large distance asymptotics because via Fourier transform they give the behaviour of the MDF for $k \sim 0$. In the bosonic case, $\kappa = 1$, the first term in the right hand-side of (70) is dominant and we have $g^{(-)}(x, 0) \sim a/x^{1/2}$ which results in an MDF behaving like $n(k) \sim 1/k^{1/2}$ for $k \rightarrow 0$ [108–111]. For free fermions, $\kappa = 0$, both terms are relevant and they reproduce the well known result $g^{(-)}(x, 0) = \sin(k_F x)/\pi x$ with $n(k) \sim \mathbf{1}_{[-k_F, k_F]}$.

The large distance asymptotics for homogeneous impenetrable Gaudin-Yang anyons is given by [27] ($\nu = -i\frac{\ln 2}{2\pi} - \frac{\kappa}{2}$)

$$g_\sigma^{(-)}(x, 0) \sim \frac{e^{-2i\nu k_F x}}{x^{2\nu^2+1}} [a x^{-2\nu} e^{-ik_F x} + b x^{2\nu} e^{ik_F x}], \quad x > 0, \quad (71)$$

with a, b constants which can be found in [27]. Similar to the single component case in the bosonic case the first term in the right hand-side is dominant obtaining [85]

$$g_\sigma^{(-)}(x, 0) \sim e^{-\frac{\ln 2}{\pi} k_F x} x^{-\frac{1}{2} + \frac{1}{2} \left(\frac{\ln 2}{\pi}\right)^2}, \quad (72)$$

and in the fermionic case both terms contribute with the results [25, 82–84, 87]

$$g_\sigma^{(-)}(x, 0) \sim e^{-\frac{\ln 2}{\pi} k_F x} x^{-1 + \frac{1}{2} \left(\frac{\ln 2}{\pi}\right)^2} \sin(k_F x - \ln 2 \ln x/\pi - \varphi_0), \quad (73)$$

with φ_0 a constant. The main feature of the asymptotics (72) and (73) is the presence of the exponential decreasing term $e^{-\frac{\ln 2}{\pi} k_F x}$ even though we are at zero temperature. This is a general feature of multicomponent systems in the spin-incoherent regime: in the case of a system with M components the exponential terms is $e^{-\frac{\ln M}{\pi} k_F x}$ [87]. The algebraic corrections are very close to the ones for single component systems $\frac{1}{2} \left(\frac{\ln 2}{\pi}\right)^2 \sim 0.024$ but in the fermionic case the oscillatory term has a $\ln x$ term dependence in addition to a phase. In the bosonic case this results in a MDF for the GY model which is wider and does not present the weak singularity $k^{-1/2}$ characteristic of single component bosons. In the fermionic case the opposite statement is true with the MDF for the GY model being narrower than the similar quantity for free fermions. These observations remain valid also in the case of harmonic trapping as it can be seen in the first row of Fig. 4 where we present the MDF for several values of t immediately after the Bragg pulse. One can see that the MDF for free fermions (their momenta are just the rapidities) remains almost unchanged while in the other cases we can clearly see the transfer of energy from the $\pm q, \pm 2q$ satellites to the modes between the peaks. The time evolution of the MDF is shown in the second row of Fig. 4 where it can be seen clearly that the modes between the first Bragg peaks are populated very rapidly. This is due to the fact that these modes are composed of the widest range of rapidities and, hence, they dephase fastest. One can see that the process of hydrodynamization takes place on the timescale set by $T_{hd} = 2\pi/\omega_{hd}$. The rapid change in the energy distribution associated with hydrodynamization can be seen more clearly by integrating the kinetic energy in successive momentum ranges and plotted as function of time as it can be seen in the last row of Fig. 4. Each curve presents the time evolution of the integrated energy in $0.1q$ wide momentum groups up to the first Bragg peak. For the GY model one can see that the rapid initial change in the intermediate momentum groups is more dramatic in the bosonic case compared with the fermionic case which is to be expected due to the wider initial MDF in the fermionic case. The change is also more pronounced in the bosonic LL model compared with the bosonic GY model due to the quasi-condensate nature of the MDF in the single component case compared with the wider MDF of the spin-incoherent GY model. While the changes in the free fermionic case are extremely small it should be noted that they are nonzero.

In Fig. 5 we present results the time evolution of the MDF and densities for a system of $N = 30$ particles at zero temperature for both the GY model and its single component counterpart and three values of the statistics parameter: $\kappa = 1$ (bosons), $\kappa = 0.5$ and $\kappa = 0$ (fermions). For $\kappa = 0.5$ one can see the nonsymmetric momentum distribution and that at $t = 0$ the MDF of the single component is narrower (the leading term comes from the Fourier transform of $e^{ik_F(\kappa-1)x}/x^{1-\kappa+\frac{\kappa^2}{2}}$) than the one for the two-component system. The nonsymmetry remains visible for the entire period of the oscillation. From the first three columns of Fig. 5 we see that the overlap between the MDF for single and two-component systems during the oscillations is pretty large with significant differences occurring in the vicinities of $t = p\pi/\omega$ and $t = \frac{1}{2}p\pi/\omega$ with p integer. However, we should point out that the tails of the MDFs which behave like $n(k, t) \sim C(t)/k^4$ with $C(t)$ the Tan contact are different with the contacts for the two-component systems being smaller than the contacts for the single component ones [85]. The density for systems with the same number of particles is independent of statistics and the number of components in the system. Its dynamics is shown in the fourth column of Fig. 5 where it can be seen that it oscillates in out-of-phase with respect to the MDFs: the density is narrowest when the MDF is largest and the converse is also true.

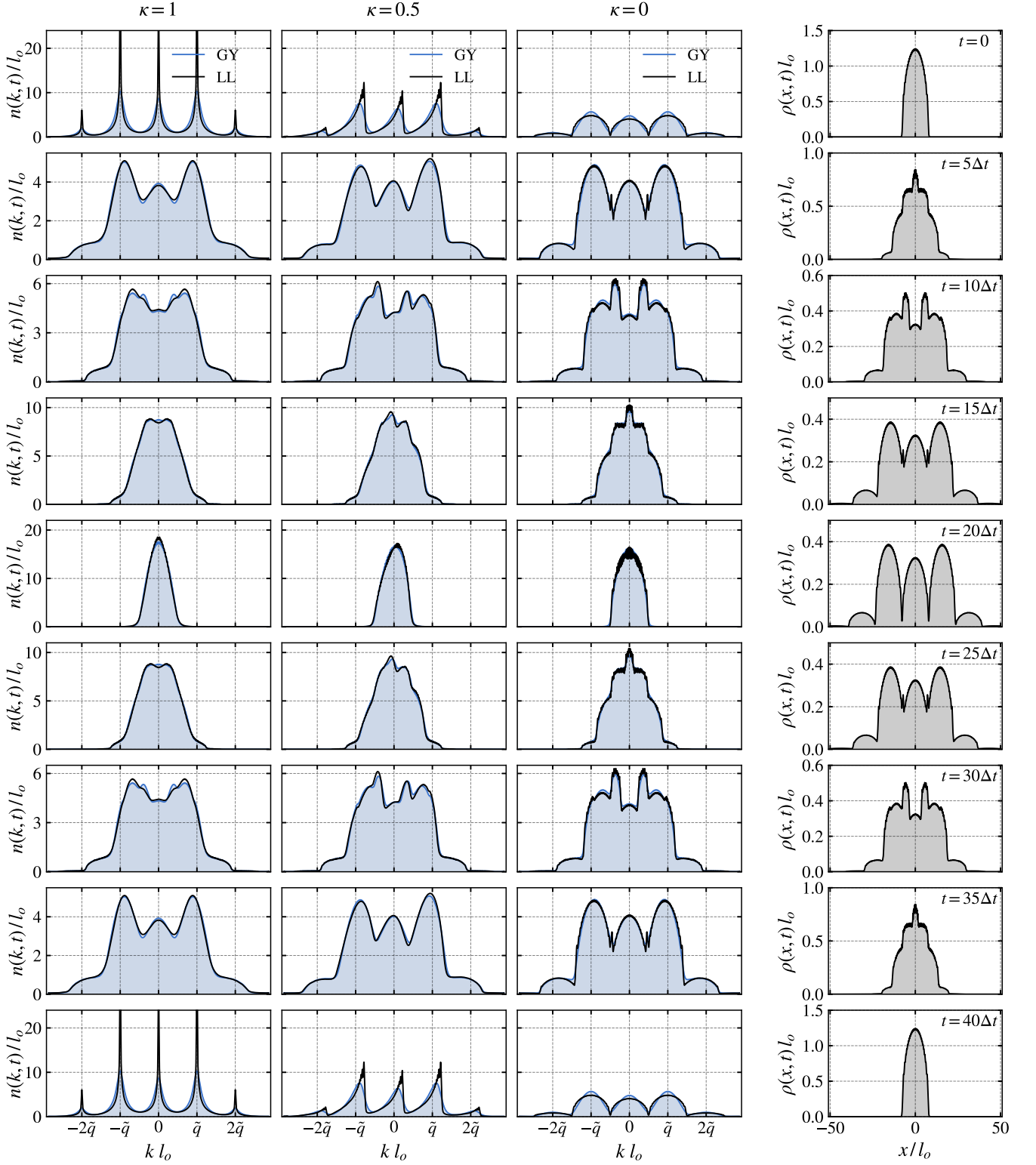


FIG. 5. Momentum distribution functions and densities of the GY and LL anyonic models for $t = \{0, 5, 10, 15, 20, 25, 30, 35, 40\} \times \Delta t$, $\Delta t = \pi/40\omega$ in the QNC setup a for a system of $N = 30$ particles at zero temperature ($\omega = 1$, $A = 1.5$, $q = 5\pi$, $l_0 = 1$, $\tilde{q} = ql_0$). First column $\kappa = 1$ (bosons), second column $\kappa = 0.5$, third column $\kappa = 0$ (fermions). Fourth column: Density which is the same for all values of κ and for both GY and LL models. The quantities for the GY model are computed using Eqs. (43), (45) and (67).

IX. CONCLUSIONS

In this paper we have investigated the nonequilibrium dynamics of the Gaudin-Yang model in two experimentally accessible scenarios: the quench induced by the sudden change in the trap's frequency and the quantum Newton's cradle setup. Our investigation used a determinant representation for the space-, time-, and temperature-dependent correlators which is extremely easy to implement numerically with the main computational effort coming from the calculation of the partial overlaps for the time evolved single particle orbitals. When the model is subjected to a quench of the trap's frequency we have identified a collective many-body bounce effect with an amplitude that depends on the statistics of the particles and for the QNC setup we have performed a thorough study of the dynamics and hydrodynamization. A natural extension of our work would be the derivation of similar representations for the lattice analog of the GY model, the Hubbard model. This will be deferred to a future publication.

ACKNOWLEDGMENTS

Financial support from the Grant No. 30N/2023 of the National Core Program of the Romanian Ministry of Research, Innovation and Digitization is gratefully acknowledged.

Appendix A: Derivation of the determinant representation for the form factors

In this Appendix we will derive the determinant representations for the form factors (26). The arbitrary state in the $(N+1, M)$ -sector appearing in the definition of the form factor is characterized by $\mathbf{j} = (j_1, \dots, j_{N+1})$ which describes the charge degrees of freedom and $\boldsymbol{\lambda} = (\lambda_1, \dots, \lambda_M)$ specifying the spin sector with $e^{i\lambda_a(N+1)} = (-1)^{M-1}$ for $a = 1, 2, \dots, M$. The other state appearing in the definition of the form factor belongs to the (N, \bar{M}) -sector and is characterized by $\mathbf{q} = (q_1, \dots, q_N)$ and $\boldsymbol{\mu} = (\mu_1, \dots, \mu_{\bar{M}})$ with $e^{i\mu_b N} = (-1)^{\bar{M}-1}$ for $b = 1, 2, \dots, \bar{M}$. Introducing

$$\Lambda = \sum_{a=1}^M \lambda_a, \quad \Theta = \sum_{b=1}^{\bar{M}} \mu_b \quad \text{and} \quad \omega = e^{i\Lambda}, \quad \nu = e^{i\Theta}, \quad (\text{A1})$$

we have

$$\eta_{N+1, M}^{(\boldsymbol{\alpha}, \alpha_1 \alpha_2 \dots \alpha_{N+1})}(\boldsymbol{\lambda}) = \omega \eta_{N+1, M}^{(\boldsymbol{\alpha}, \alpha_2 \alpha_3 \dots \alpha_{N+1} \alpha_1)}(\boldsymbol{\lambda}), \quad (\text{A2})$$

$$\eta_{N, \bar{M}}^{(\boldsymbol{\alpha}, \alpha_1 \alpha_2 \dots \alpha_N)}(\boldsymbol{\mu}) = \nu \eta_{N, \bar{M}}^{(\boldsymbol{\alpha}, \alpha_2 \alpha_3 \dots \alpha_N \alpha_1)}(\boldsymbol{\mu}), \quad (\text{A3})$$

which is a consequence of the fact that the XX spin chain wavefunctions (9) are also eigenfunctions of the cyclic shift operator on the lattice. Also, using (13) we obtain

$$\mathcal{F}_{N, M}^{(\sigma)}(\mathbf{j}, \boldsymbol{\lambda}; \mathbf{q}, \boldsymbol{\mu} | x, t) = e^{it\mu\sigma} \langle \Psi_{N, \bar{M}}(t | \mathbf{q}, \boldsymbol{\mu}) | \Psi_{\sigma}(x) | \Phi_{N+1, M}(t | \mathbf{j}, \boldsymbol{\lambda}) \rangle, \quad (\text{A4})$$

with the time evolved wavefunctions given by (14) and $\mu_{\uparrow} = \mu - B$, $\mu_{\downarrow} = \mu + B$. Using the commutation relations (2) and the symmetry of the wavefunctions (11) the starting point of our calculations is

$$\mathcal{F}_{N, M}^{(\sigma)}(x, t) = (N+1)! e^{it\mu\sigma} \int_{L_-}^{L_+} \prod_{i=1}^N dx_i \sum_{\alpha_1, \dots, \alpha_N = \{\uparrow, \downarrow\}}^{[N, \bar{M}]} \bar{\chi}_{N, \bar{M}}^{\boldsymbol{\alpha}}(x_1, \dots, x_N, t | \mathbf{q}, \boldsymbol{\mu}) \chi_{N+1, M}^{\boldsymbol{\alpha}\sigma}(x_1, \dots, x_N, x, t | \mathbf{j}, \boldsymbol{\lambda}) \quad (\text{A5})$$

where the bar denotes complex conjugation and L_{\pm} are the limits of integration which can differ depending on the system we consider. For example, in the case of trapping we have $L_{\pm} = \pm\infty$ but in the case of Dirichlet boundary conditions in the box $[0, L]$ we have $L_- = 0$ and $L_+ = L$. The evolved wavefunctions are

$$\begin{aligned} \bar{\chi}_{N, \bar{M}}^{\boldsymbol{\alpha}}(x_1, \dots, x_N, t | \mathbf{q}, \boldsymbol{\mu}) &= \frac{1}{N! N^{\bar{M}/2}} \left[\sum_{R \in S_N} \theta(R\mathbf{x}) e^{-i\frac{\pi\kappa}{2} \sum_{1 \leq a < b < N} \text{sign}(x_a - x_b)} \bar{\eta}_{N, \bar{M}}^{(\boldsymbol{\alpha}, R\boldsymbol{\alpha})}(\boldsymbol{\mu}) \right] \\ &\quad \times \sum_{Q \in S_N} (-1)^Q \prod_{l=1}^N \bar{\phi}_{qQ(l)}(x_l, t), \end{aligned} \quad (\text{A6})$$

and

$$\chi_{N+1,M}^{\alpha\sigma}(x_1, \dots, x_N, x, t | \mathbf{j}, \boldsymbol{\lambda}) = \frac{1}{(N+1)!(N+1)^{M/2}} \left[\sum_{R' \in S_{N+1}} \theta(R' \mathbf{x}') e^{i \frac{\pi\kappa}{2} \sum_{1 \leq a < b < N} \text{sign}(x_a - x_b)} e^{i \frac{\pi\kappa}{2} \sum_{a=1}^N \text{sign}(x_a - x)} \right. \\ \left. \times \eta_{N+1,M}^{(\alpha\sigma, R' \alpha\sigma)}(\boldsymbol{\lambda}) \right] \sum_{P \in S_{N+1}} (-1)^P \prod_{l=1}^N \phi_{j_{P(l)}}(x_l, t) \phi_{j_{P(N+1)}}(x, t), \quad (\text{A7})$$

where $R\mathbf{x} = x_{R(1)} < \dots < x_{R(N)}$ and $R'\mathbf{x}' = x_{R'(1)} < \dots < x_{R'(N+1)}$ (one $x_{R'(i)} = x$). Multiplying the wavefunctions we encounter products of the type $\theta(R\mathbf{x})\theta(R'\mathbf{x}') = \prod_{j=1}^N \delta_{R(j), R'(j)} \theta(R'\mathbf{x}')$ with $R \in S_N$ and $R' \in S_{N+1}$. The $(N+1)!$ surviving terms can be divided in $N+1$ sets of $N!$ terms depending on the position of $R'(N+1)$ which indexes the position of x i.e.,

$$\sum_{R \in S_N} \sum_{R' \in S_{N+1}} \theta(R\mathbf{x})\theta(R'\mathbf{x}') = \sum_{R \in S_N} \left\{ \theta(x_{R(1)} < \dots < x_{R(N)} < x) \right. \\ \left. + \sum_{n=1}^{N-1} \theta(x_{R(1)} < \dots < x_{R(n)} < x < x_{R(n+1)} < \dots < x_{R(N)}) \right. \\ \left. + \theta(x < z_{R(1)} < \dots < x_{R(N)}) \right\}. \quad (\text{A8})$$

If we consider the set in which x is on the n -th position, then, for a given $\boldsymbol{\alpha} = (\alpha_1 \dots \alpha_N)$, the product of spin wavefunctions is given by $\bar{\eta}_{N,\bar{M}}^{(\boldsymbol{\alpha}, R\boldsymbol{\alpha})}(\boldsymbol{\mu}) \eta_{N+1,M}^{(\boldsymbol{\alpha}\sigma, R' \boldsymbol{\alpha}\sigma)}(\boldsymbol{\lambda}) = \bar{\eta}_{N,\bar{M}}^{(\boldsymbol{\alpha}, \alpha_1 \dots \alpha_N)}(\boldsymbol{\mu}) \eta_{N+1,M}^{(\boldsymbol{\alpha}\sigma, \alpha_1 \dots \alpha_n \sigma \alpha_{n+1} \dots \alpha_N)}(\boldsymbol{\lambda})$. Collecting these results (A4) can be written as

$$\mathcal{F}_{N,M}^{(\sigma)}(x, t) = \frac{e^{it\mu_\sigma}}{N!N^{\bar{M}/2}(N+1)^{M/2}} \int_{L_-}^{L_+} \prod_{i=1}^N dx_i \sum_{R \in S_N} \left\{ \theta(x_{R(1)} < \dots < x_{R(N)} < x) e^{-i \frac{\pi\kappa}{2} N} F_\sigma(N) \right. \\ \left. + \sum_{n=1}^{N-1} \theta(x_{R(1)} < \dots < x_{R(n)} < x < x_{R(n+1)} < \dots < x_{R(N)}) e^{-i \frac{\pi\kappa}{2} n} e^{i \frac{\pi\kappa}{2} (N-n)} F_\sigma(n) \right. \\ \left. + \theta(x < z_{R(1)} < \dots < x_{R(N)}) e^{i \frac{\pi\kappa}{2} N} F_\sigma(0) \right\} \left(\sum_{Q \in S_N} (-1)^Q \prod_{l=1}^N \bar{\phi}_{q_{Q(l)}}(x_l, t) \right) \\ \times \left(\sum_{P \in S_{N+1}} (-1)^P \prod_{l=1}^N \phi_{j_{P(l)}}(x_l, t) \phi_{j_{P(N+1)}}(x, t) \right), \quad (\text{A9})$$

with

$$F_\sigma(n) = \sum_{\alpha_1, \dots, \alpha_N = \{\uparrow, \downarrow\}}^{[N, \bar{M}]} \bar{\eta}_{N,\bar{M}}^{(\boldsymbol{\alpha}, \alpha_1 \dots \alpha_N)}(\boldsymbol{\mu}) \eta_{N+1,M}^{(\boldsymbol{\alpha}\sigma, \alpha_1 \dots \alpha_n \sigma \alpha_{n+1} \dots \alpha_N)}(\boldsymbol{\lambda}). \quad (\text{A10})$$

Using the cyclic property of the spin wavefunctions (A2) and the fact that $\bar{\omega} = \omega^{-1}$, $\bar{\nu} = \nu^{-1}$ we find that

$$F_\sigma(n) = (\bar{\omega}\nu)^{N-n} F_\sigma(N), \quad F_\sigma \equiv F_\sigma(N), \quad (\text{A11})$$

and, therefore,

$$\mathcal{F}_{N,M}^{(\sigma)}(x, t) = \frac{e^{it\mu_\sigma} e^{-i \frac{\pi\kappa}{2} N} F_\sigma}{N!N^{\bar{M}/2}(N+1)^{M/2}} \int_{L_-}^{L_+} \prod_{i=1}^N dx_i \sum_{R \in S_N} \left\{ \theta(x_{R(1)} < \dots < x_{R(N)} < x) \right. \\ \left. + \sum_{n=1}^{N-1} \theta(x_{R(1)} < \dots < x_{R(n)} < x < x_{R(n+1)} < \dots < x_{R(N)}) (\bar{\omega}\nu e^{i\pi\kappa})^{N-n} \right. \\ \left. + \theta(x < z_{R(1)} < \dots < x_{R(N)}) (\bar{\omega}\nu e^{i\pi\kappa})^N \right\} \left(\sum_{Q \in S_N} (-1)^Q \prod_{l=1}^N \bar{\phi}_{q_{Q(l)}}(x_l, t) \right)$$

$$\times \left(\sum_{P \in S_{N+1}} (-1)^P \prod_{l=1}^N \phi_{j_{P(l)}}(x_l, t) \phi_{j_{P(N+1)}}(x, t) \right). \quad (\text{A12})$$

Fortunately, one can show that

$$\sum_{R \in S_N} \left\{ \theta(x_{R(1)} < \dots < x_{R(N)} < x) + \sum_{n=1}^{N-1} \theta(x_{R(1)} < \dots < x_{R(n)} < x < x_{R(n+1)} < \dots < x_{R(N)}) (\bar{\omega} \nu e^{i\pi\kappa})^{N-n} \right. \\ \left. + \theta(x < x_{R(1)} < \dots < x_{R(N)}) (\bar{\omega} \nu e^{i\pi\kappa})^N \right\} = \prod_{n=1}^N \rho(x - x_n), \quad (\text{A13})$$

with

$$\rho(x) = \theta(x) + e^{i\pi\kappa} \bar{\omega} \nu \theta(-x). \quad (\text{A14})$$

This identity is valid for all $x_1, \dots, x_N \in [L_-, L_+]$ when the x_i 's are different. The value of $\rho(0)$ is not important because when two coordinates are equal the determinants in the right hand-side of (A12) vanish. In order to prove this identity it is instructive to look at the particular case $N = 2$ where the left hand side of (A13) is

$$L.H.S = \sum_{R \in S_2} \left\{ \theta(x_{R(1)} < x_{R(2)} < x) + \theta(x_{R(1)} < x < x_{R(2)}) \bar{\omega} \nu e^{i\pi\kappa} + \theta(x < x_{R(1)} < x_{R(2)}) (\bar{\omega} \nu e^{i\pi\kappa})^2 \right\} \quad (\text{A15})$$

and the right hand side is

$$R.H.S = \theta(x - x_1)\theta(x - x_2) + [\theta(x - x_1)\theta(x_2 - x) + \theta(x - x_2)\theta(x_1 - x)] \bar{\omega} \nu e^{i\pi\kappa} + \theta(x_1 - x)\theta(x_2 - x) (\bar{\omega} \nu e^{i\pi\kappa})^2. \quad (\text{A16})$$

The equality of (A15) and (A16) becomes evident noticing that $\theta(x - x_1)\theta(x - x_2) = \sum_{R \in S_2} \theta(x_{R(1)} < x_{R(2)} < x)$, $[\theta(x - x_1)\theta(x_2 - x) + \theta(x - x_2)\theta(x_1 - x)] = \sum_{R \in S_2} \theta(x_{R(1)} < x < x_{R(2)})$ and $\theta(x_1 - x)\theta(x_2 - x) = \sum_{R \in S_2} \theta(x < x_{R(1)} < x_{R(2)})$. The general case is proved along the same lines by noticing that the terms multiplied by $(\bar{\omega} \nu e^{i\pi\kappa})^{N-n}$ obtained by expanding the r.h.s of (A13) are equal to $\sum_{R \in S_N} \theta(x_{R(1)} < \dots < x_{R(n)} < x < x_{R(n+1)} < \dots < x_{R(N)})$.

Inserting the identity (A13) in (A12) we see that the integration over the charge degrees of freedom can be written in a factorized form

$$\mathcal{F}_{N,M}^{(\sigma)}(x, t) = \frac{e^{it\mu\sigma} e^{-i\frac{\pi\kappa N}{2}} F_\sigma}{N! N^{M/2} (N+1)^{M/2}} \int_{L_-}^{L_+} \prod_{i=1}^N dx_i \rho(x - x_i) \sum_{Q \in S_N} \sum_{P \in S_{N+1}} (-1)^{P+Q} \left(\prod_{l=1}^N \bar{\phi}_{q_{Q(l)}}(x_l, t) \phi_{j_{P(l)}}(x_l, t) \right) \\ \times \phi_{j_{P(N+1)}}(x, t). \quad (\text{A17})$$

Using the orthonormality of the wavefunctions $\int_{L_-}^{L_+} \bar{\phi}_q(v, t) \phi_j(v, t) dv = \delta_{j,q}$ the integrals over x_i can be calculated using the formula

$$\int_{L_-}^{L_+} \rho(x - v) \bar{\phi}_q(v, t) \phi_j(v, t) dv = \int_{L_-}^x \bar{\phi}_q(v, t) \phi_j(v, t) dv + e^{i\pi\kappa} \bar{\omega} \nu \int_x^{L_+} \bar{\phi}_q(v, t) \phi_j(v, t) dv, \\ = \int_{L_-}^{L_+} \bar{\phi}_q(v, t) \phi_j(v, t) dv - (1 - e^{i\pi\kappa} \bar{\omega} \nu) \int_x^{L_+} \bar{\phi}_q(v, t) \phi_j(v, t) dv, \\ = f(j, q|x, t),$$

with

$$f(j, q|x, t) = \delta_{j,q} - (1 - e^{i\pi\kappa} \bar{\omega} \nu) \int_x^{L_+} \bar{\phi}_q(v, t) \phi_j(v, t) dv. \quad (\text{A18})$$

Therefore, we find

$$\mathcal{F}_{N,M}^{(\sigma)}(x, t) = \frac{e^{it\mu\sigma} e^{-i\frac{\pi\kappa N}{2}} F_\sigma}{N! N^{M/2} (N+1)^{M/2}} \sum_{Q \in S_N} \sum_{P \in S_{N+1}} (-1)^{P+Q} \left(\prod_{l=1}^N f(j_{P(l)}, q_{Q(l)}|x, t) \right) \phi_{j_{P(N+1)}}(x, t), \quad (\text{A19})$$

with the last part which can be written as a determinant

$$\sum_{Q \in S_N} (-1)^Q \begin{vmatrix} f(j_1, q_{Q(1)}) & \cdots & f(j_1, q_{Q(N)}) & \phi_{j_1} \\ \vdots & \ddots & \vdots & \vdots \\ f(j_{N+1}, q_{Q(1)}) & \cdots & f(j_{N+1}, q_{Q(N)}) & \phi_{j_{N+1}} \end{vmatrix} (x, t). \quad (\text{A20})$$

Reorganizing the columns such that $(Q_1, \dots, Q_N) \rightarrow (1, \dots, N)$ gives a $(-1)^Q$ sign, therefore, the sum produces $N!$ identical terms and the form factor can be written as

$$\mathcal{F}_{N,M}^{(\sigma)}(x, t) = \frac{e^{it\mu\sigma} e^{-i\frac{\pi k N}{2}}}{N^{\bar{M}/2} (N+1)^{M/2}} F_\sigma \det_{N+1} D(\mathbf{j}, \mathbf{q}|x, t), \quad (\text{A21})$$

with $D(\mathbf{j}, \mathbf{q}|x, t)$ a square matrix of dimension $N+1$ and elements

$$[D(\mathbf{j}, \mathbf{q}|x, t)]_{ab} = \begin{cases} f(j_a, q_b|x, t) & \text{for } a = 1, \dots, N+1; b = 1, \dots, N, \\ \phi_{j_a}(x, t) & \text{for } a = 1, \dots, N+1; b = N+1. \end{cases} \quad (\text{A22})$$

The only thing that remains is to compute is the F_σ factor. We start with the case $\sigma = \uparrow$. Taking into account that the n 's are the position of the spin down particles on the lattice the first observation that we make is that the sum over α 's in

$$F_\sigma \equiv F_\sigma(N) = \sum_{\alpha_1, \dots, \alpha_N = \{\uparrow, \downarrow\}}^{[N, \bar{M}]} \bar{\eta}_{N, \bar{M}}^{(\alpha, \alpha_1 \dots \alpha_N)}(\boldsymbol{\mu}) \eta_{N+1, M}^{(\alpha\sigma, \alpha_1 \dots \alpha_N \sigma)}(\boldsymbol{\lambda}). \quad (\text{A23})$$

is equivalent with $\sum_{1 \leq n_1 < \dots < n_M \leq N}$. For $\sigma = \uparrow$ the product $\bar{\eta}_{N, \bar{M}} \eta_{N+1, M}$ is symmetric in n 's (the products of sign factors cancel) and vanish when two of them are equal. Therefore, we have

$$\sum_{1 \leq n_1 < \dots < n_M \leq N} = \frac{1}{M!} \sum_{n_1=1}^N \cdots \sum_{n_M=1}^N, \quad (\text{A24})$$

and

$$\begin{aligned} F_\uparrow &= \frac{1}{M!} \sum_{n_1=1}^N \cdots \sum_{n_M=1}^N \left(\sum_{Q \in S_M} (-1)^Q \prod_{k=1}^M e^{-in_k \mu_{Q(k)}} \right) \left(\sum_{P \in S_M} (-1)^P \prod_{k=1}^M e^{in_k \lambda_{P(k)}} \right), \\ &= \frac{1}{M!} \sum_{n_1=1}^N \cdots \sum_{n_M=1}^N \sum_{Q \in S_M} \sum_{P \in S_M} (-1)^{P+Q} \prod_{k=1}^M e^{in_k (\lambda_{P(k)} - \mu_{Q(k)})}, \\ &= \sum_{P \in S_M} (-1)^P \prod_{k=1}^M \left(\sum_{n=1}^N e^{in(\lambda_{P(k)} - \mu_j)} \right), \end{aligned} \quad (\text{A25})$$

which shows that $F_\uparrow = \det_M B_\uparrow(\boldsymbol{\lambda}, \boldsymbol{\mu})$ where the matrix B_\uparrow has elements. In the $\sigma = \downarrow$ case we have $\bar{M} = M-1$ and $n_M = N+1$ for the n 's in $\eta_{N+1, M}^{(\alpha\sigma, \alpha_1 \dots \alpha_N \sigma)}(\boldsymbol{\lambda})$. The the product $\bar{\eta}_{N, \bar{M}} \eta_{N+1, M}$ is now symmetric in $M-1$ variables and vanish when two of them are equal. We find

$$\begin{aligned} F_\downarrow &= \frac{1}{(M-1)!} \sum_{n_1=1}^N \cdots \sum_{n_{M-1}=1}^N \left(\sum_{Q \in S_{M-1}} (-1)^Q \prod_{k=1}^{M-1} e^{-in_k \mu_{Q(k)}} \right) \left(\sum_{P \in S_M} (-1)^P \prod_{k=1}^{M-1} e^{in_k \lambda_{P(k)}} \right) e^{i(N+1)\lambda_{P(M)}}, \\ &= \frac{1}{(M-1)!} \sum_{n_1=1}^N \cdots \sum_{n_{M-1}=1}^N \sum_{Q \in S_{M-1}} \sum_{P \in S_M} (-1)^{P+Q} \prod_{k=1}^M e^{in_k (\lambda_{P(k)} - \mu_{Q(k)})} (-1)^{M-1}, \\ &= \frac{1}{(M-1)!} \sum_{Q \in S_{M-1}} \sum_{P \in S_M} (-1)^{P+Q} \prod_{k=1}^M \left(\sum_{n=1}^N e^{in(\lambda_{P(k)} - \mu_{Q(k)})} \right) (-1)^{M-1}, \end{aligned} \quad (\text{A26})$$

where in the second line we have used the BAEs $e^{i\lambda_a(N+1)} = (-1)^{M-1}$. The analysis of the last expression is similar with the one for the charge degrees of freedom. We obtain $F_\downarrow = (-1)^{M-1} \det_M B_\downarrow(\boldsymbol{\lambda}, \boldsymbol{\mu})$ with matrix elements

$$[B_\downarrow(\boldsymbol{\lambda}, \boldsymbol{\mu})]_{ab} = \begin{cases} \sum_{n=1}^N e^{in(\lambda_a - \mu_b)} & \text{for } a = 1, \dots, M; b = 1, \dots, M-1, \\ 1 & \text{for } a = 1, \dots, M; b = M. \end{cases} \quad (\text{A27})$$

Appendix B: Derivation of the determinant representation for the correlators

Here, we present the derivation of the determinant representation for the correlators starting with the summation of form factors for the mean values appearing on the right hand side of (17) and (18).

1. Determinant representation for $\langle \Phi_{N+1,M}(\mathbf{j}, \boldsymbol{\lambda}) | \Psi_{\uparrow}^{\dagger}(x, t) \Psi_{\uparrow}(y, t') | \Phi_{N+1,M}(\mathbf{j}, \boldsymbol{\lambda}) \rangle$

Using the determinant formulas for the form factors (26) one can obtain similar representations for the mean value of bilocal operators appearing in the definition of the correlators (17) and (18). In this section we consider $A \equiv \langle \Phi_{N+1,M}(\mathbf{j}, \boldsymbol{\lambda}) | \Psi_{\uparrow}^{\dagger}(x, t) \Psi_{\uparrow}(y, t') | \Phi_{N+1,M}(\mathbf{j}, \boldsymbol{\lambda}) \rangle$. In this case $\bar{M} = M$ and we have

$$\begin{aligned} A &= \sum_{\substack{q_1 < \dots < q_N \\ \mu_1 < \dots < \mu_M}} \bar{\mathcal{F}}_{N,M}^{(\uparrow)}(\mathbf{j}, \boldsymbol{\lambda}; \mathbf{q}, \boldsymbol{\mu} | x, t) \mathcal{F}_{N,M}^{(\uparrow)}(\mathbf{j}, \boldsymbol{\lambda}; \mathbf{q}, \boldsymbol{\mu} | y, t'), \\ &= \sum_{\substack{q_1 < \dots < q_N \\ \mu_1 < \dots < \mu_M}} \frac{e^{-i(t-t')\mu_{\uparrow}}}{(N+1)^M N^M} |\det B_{\uparrow}(\boldsymbol{\lambda}, \boldsymbol{\mu})|_M^2 \overline{\det D(\mathbf{j}, \mathbf{q} | x, t)}_{N+1} \det D(\mathbf{j}, \mathbf{q} | y, t')_{N+1}. \end{aligned} \quad (\text{B1})$$

In (B1) the summation over q 's is independent on the summation on μ 's and the summands are symmetric functions independently in q 's and μ 's and vanish when two of them are equal (exchanging two q 's is equivalent with transposing two columns in the matrix D and we have a product of $\bar{D}D$, the same argument applies in the case of exchange of two μ 's). Therefore, the summations can be written as

$$\sum_{\substack{q_1 < \dots < q_N \\ \mu_1 < \dots < \mu_M}} = \frac{1}{N!} \sum_{q_1=1}^{\infty} \dots \sum_{q_N=1}^{\infty} \frac{1}{M!} \sum_{\mu_1} \dots \sum_{\mu_M} \quad (\text{B2})$$

where $\sum_{\mu} h(\mu) = \sum_{l=1}^N h(\mu_l)$ with $\mu_l = \frac{2\pi}{N} \left(-\frac{N}{2} - \frac{1+(-1)^{N-M}}{4} + l \right)$ for an arbitrary function h .

a. Summation over q_1, \dots, q_N

We focus now on the summation over the q 's in (B1). We find

$$\begin{aligned} A_q &= \frac{1}{N!} \sum_{q_1=1}^{\infty} \dots \sum_{q_N=1}^{\infty} \frac{\det D(\mathbf{j}, \mathbf{q} | x, t)}{N+1} \det D(\mathbf{j}, \mathbf{q} | y, t')_{N+1} \\ &= \frac{1}{N!} \sum_{q_1=1}^{\infty} \dots \sum_{q_N=1}^{\infty} \sum_{P \in S_{N+1}} \sum_{Q \in S_{N+1}} (-1)^{P+Q} \left(\prod_{l=1}^N \bar{f}(j_{P(l)}, q_l | x, t) f(j_{Q(l)}, q_l | y, t') \right) \bar{\phi}_{j_{P(N+1)}}(x, t) \phi_{j_{Q(N+1)}}(y, t'), \\ &= \frac{1}{N!} \sum_{q_1=1}^{\infty} \dots \sum_{q_N=1}^{\infty} \sum_{R, Q \in S_{N+1}} (-1)^R \left(\prod_{l=1}^N \bar{f}(j_{RQ(l)}, q_l | x, t) f(j_{Q(l)}, q_l | y, t') \right) \bar{\phi}_{j_{RQ(N+1)}}(x, t) \phi_{j_{Q(N+1)}}(y, t'), \end{aligned} \quad (\text{B3})$$

where in the last line we have used the fact that every permutation P can be written as $P = RQ$ with R another permutation. The sum over permutations in (B3) can be written as a sum over determinants

$$\sum_{Q \in S_{N+1}} \left| \begin{array}{cccc} \bar{f}(j_{Q(1)}, q_1 | x, t) f(j_{Q(1)}, q_1 | y, t') & \dots & \bar{f}(j_{Q(1)}, q_N | x, t) f(j_{Q(N)}, q_N | y, t') & \bar{\phi}_{j_{Q(1)}}(x, t) \phi_{j_{Q(N+1)}}(y, t') \\ \vdots & \ddots & \vdots & \vdots \\ \bar{f}(j_{Q(N+1)}, q_1 | x, t) f(j_{Q(1)}, q_1 | y, t') & \dots & \bar{f}(j_{Q(N+1)}, q_N | x, t) f(j_{Q(N)}, q_N | y, t') & \bar{\phi}_{j_{Q(N+1)}}(x, t) \phi_{j_{Q(N+1)}}(y, t') \end{array} \right|$$

In the previous result q_i appears only in the i -th column which means that we can sum inside the determinant. Introducing two square matrices of dimension $N+1$, depending on the state \mathbf{j} , with elements

$$\tilde{U}_{ab}^{(-)}(x, t; y, t') = \sum_{q=1}^{\infty} \bar{f}(j_a, q | x, t) f(j_b, q | y, t'), \quad a, b = 1, \dots, N+1, \quad (\text{B4})$$

$$\tilde{R}_{ab}^{(-)}(x, t; y, t') = \bar{\phi}_{j_a}(x, t)\phi_{j_b}(y, t'), \quad a, b = 1, \dots, N+1 \quad (\text{B5})$$

we obtain

$$A_q = \frac{1}{N!} \sum_{Q \in S_{N+1}} \begin{vmatrix} \tilde{U}_{Q(1), Q(1)}^{(-)} & \cdots & \tilde{U}_{Q(1), Q(N)}^{(-)} & \tilde{R}_{Q(1), Q(N+1)}^{(-)} \\ \vdots & \ddots & \vdots & \vdots \\ \tilde{U}_{Q(N+1), Q(1)}^{(-)} & \cdots & \tilde{U}_{Q(N+1), Q(N)}^{(-)} & \tilde{R}_{Q(N+1), Q(N+1)}^{(-)} \end{vmatrix} (x, t; y, t'). \quad (\text{B6})$$

Performing permutations of both columns and rows such that $(Q(1), \dots, Q(N+1)) \rightarrow (1, \dots, N+1)$ we find

$$A_q = \sum_{k=1}^{N+1} \begin{vmatrix} \tilde{U}_{1,1}^{(-)} & \cdots & \tilde{R}_{1,k}^{(-)} & \tilde{U}_{1,N+1}^{(-)} \\ \vdots & \ddots & \vdots & \vdots \\ \tilde{U}_{N+1,1}^{(-)} & \cdots & \tilde{R}_{N+1,k}^{(-)} & \tilde{U}_{N+1,N+1}^{(-)} \end{vmatrix} (x, t; y, t'). \quad (\text{B7})$$

which can be written as

$$A_q = \frac{\partial}{\partial z} \det_{N+1} \left(\tilde{U}^{(-)} + z\tilde{R}^{(-)} \right) \Big|_{z=0}, \quad (\text{B8})$$

$$= \det_{N+1} \left(\tilde{U}^{(-)} + \tilde{R}^{(-)} \right) - \det_{N+1} \tilde{U}^{(-)}, \quad (\text{B9})$$

due to the fact that the matrix $\tilde{R}^{(-)}$ has rank 1.

b. Summation over μ_1, \dots, μ_M

We have obtained that

$$A = \frac{1}{M!} \sum_{\mu_1} \cdots \sum_{\mu_M} \frac{e^{-i(t-t')\mu_\uparrow}}{(N+1)^M N^M} |\det_M B_\uparrow(\boldsymbol{\lambda}, \boldsymbol{\mu})|^2 \left[\det_{N+1} \left(\tilde{U}^{(-)} + \tilde{R}^{(-)} \right) - \det_{N+1} \tilde{U}^{(-)} \right], \quad (\text{B10})$$

where the term appearing in the square parenthesis depends on μ_1, \dots, μ_M only via $e^{i\Theta} = e^{i\sum_{a=1}^M \mu_a}$ [see (A18) and (B4)]. This also means that the square parenthesis is periodic on Θ with period 2π . Because $e^{i\mu_b N} = (-1)^{\overline{M-1}}$ or, equivalently, because $e^{i\Theta}$ are eigenvalues of the cyclic shift operator we have $\Theta = \frac{2\pi n}{N}$ with $n = 0, 1, \dots, N-1$. Therefore, in terms of the Kronecker symbol on \mathbb{Z}_N defined by

$$\delta_{(N)}(m) = \begin{cases} 1 & \text{if } m = 0 \pmod{N}, \\ 0 & \text{otherwise,} \end{cases} \quad \delta_{(N)}(m) = \frac{1}{N} \sum_{p=0}^{N-1} e^{\frac{2\pi i}{N} pm}, \quad (\text{B11})$$

a resolution of unity can be written as $1 = \sum_{n=0}^{N-1} \delta_{(N)} \left(N \frac{\mu_1 + \dots + \mu_M}{2\pi} - n \right)$. Defining $\tilde{U}_n^{(-)} = \tilde{U}^{(-)}|_{\Theta=2\pi n/N}$ (note that $R^{(-)}$ does not depend on Θ) then (B10) can be written as

$$A = \frac{1}{M!} \sum_{\mu_1} \cdots \sum_{\mu_M} \frac{e^{-i(t-t')\mu_\uparrow}}{(N+1)^M N^{M+1}} \sum_{n,p=0}^{N-1} e^{ip(\mu_1 + \dots + \mu_M) - \frac{2\pi i}{N} pn} |\det_M B_\uparrow(\boldsymbol{\lambda}, \boldsymbol{\mu})|^2 \left[\det_{N+1} \left(\tilde{U}_n^{(-)} + \tilde{R}^{(-)} \right) - \det_{N+1} \tilde{U}_n^{(-)} \right], \quad (\text{B12})$$

with $[B_\uparrow(\boldsymbol{\lambda}, \boldsymbol{\mu})]_{ab} = \sum_{n=1}^N e^{in(\lambda_a - \mu_b)}$. Let us focus on

$$A_\mu = \frac{1}{M!} \sum_{\mu_1} \cdots \sum_{\mu_M} \frac{e^{ip(\mu_1 + \dots + \mu_M)}}{(N+1)^M N^{M+1}} |\det_M B_\uparrow(\boldsymbol{\lambda}, \boldsymbol{\mu})|^2. \quad (\text{B13})$$

Using the definition of the determinant we have

$$A_\mu = \frac{1}{M!} \sum_{\mu_1} \cdots \sum_{\mu_M} \frac{e^{ip(\mu_1 + \dots + \mu_M)}}{(N+1)^M N^{M+1}} \left(\sum_{P \in S_M} (-1)^P \prod_{a=1}^M [\bar{B}_\uparrow]_{P(a), a} \right) \left(\sum_{Q \in S_M} (-1)^Q \prod_{a=1}^M [B_\uparrow]_{Q(a), a} \right),$$

$$\begin{aligned}
&= \frac{1}{M!} \sum_{\mu_1} \cdots \sum_{\mu_M} \frac{e^{ip(\mu_1 + \cdots + \mu_M)}}{(N+1)^M N^{M+1}} \sum_{Q \in S_M} \sum_{R \in S_M} (-1)^R \prod_{a=1}^M \left([\overline{B}_\uparrow]_{RQ(a),a} [\overline{B}_\uparrow]_{Q(a),a} \right), \\
&= \frac{1}{M!} \sum_{\mu_1} \cdots \sum_{\mu_M} \frac{e^{ip(\mu_1 + \cdots + \mu_M)}}{(N+1)^M N^{M+1}} \sum_{Q \in S_M} \left| \begin{array}{ccc} [\overline{B}_\uparrow]_{Q(1),1} & \cdots & [\overline{B}_\uparrow]_{Q(1),M} \\ \vdots & \ddots & \vdots \\ [\overline{B}_\uparrow]_{Q(M),1} & \cdots & [\overline{B}_\uparrow]_{Q(M),M} \end{array} \right| \prod_{a=1}^M \left([\overline{B}_\uparrow]_{Q(a),a} \right), \\
&= \frac{1}{M!} \sum_{\mu_1} \cdots \sum_{\mu_M} \sum_{Q \in S_M} \left| \begin{array}{ccc} \frac{[\overline{B}_\uparrow]_{Q(1),1} [B_\uparrow]_{Q(1),1} e^{ip\mu_1}}{N(N+1)} & \cdots & \frac{[\overline{B}_\uparrow]_{Q(1),M} [B_\uparrow]_{Q(M),M} e^{ip\mu_M}}{N(N+1)} \\ \vdots & \ddots & \vdots \\ \frac{[\overline{B}_\uparrow]_{Q(M),1} [B_\uparrow]_{Q(1),1} e^{ip\mu_1}}{N(N+1)} & \cdots & \frac{[\overline{B}_\uparrow]_{Q(M),M} [B_\uparrow]_{Q(M),M} e^{ip\mu_M}}{N(N+1)} \end{array} \right|. \tag{B14}
\end{aligned}$$

In the last determinant of (B14) μ_j appears only in the j -th column so we can sum inside the determinant. Introducing a set of matrices of dimension M denoted by $O_p^{(-,\uparrow)}$ with elements

$$[O_p^{(-,\uparrow)}]_{ab} = \frac{1}{N(N+1)} \sum_{n=1}^N \sum_{m=1}^N \sum_{\mu} e^{i(p+m-n)\mu + in\lambda_a - im\lambda_b}, \quad a, b = 1, \dots, M, \tag{B15}$$

we obtain

$$A_\mu = \frac{1}{N} \frac{1}{M!} \sum_{Q \in S_M} \left| \begin{array}{ccc} [\overline{O}_p^{(\uparrow,-)}]_{Q(1),Q(1)} & \cdots & [\overline{O}_p^{(\uparrow,-)}]_{Q(1),Q(M)} \\ \vdots & \ddots & \vdots \\ [\overline{O}_p^{(\uparrow,-)}]_{Q(M),Q(1)} & \cdots & [\overline{O}_p^{(\uparrow,-)}]_{Q(M),Q(M)} \end{array} \right|. \tag{B16}$$

Permuting the rows and columns such that $(Q(1), \dots, Q(M)) \rightarrow (1, \dots, M)$ we obtain $M!$ identical terms. Plugging (B16) in (B12) we finally obtain

$$A = e^{-i(t-t')\mu_\uparrow} \frac{1}{N} \sum_{n,p=0}^{N-1} e^{-\frac{2\pi i}{N}pn} \det_M O_p^{(-,\uparrow)} \left[\det_{N+1} (\tilde{U}_n^{(-)} + \tilde{R}^{(-)}) - \det_{N+1} \tilde{U}_n^{(-)} \right], \tag{B17}$$

which represents the finite size determinant representation for the mean value $A \equiv \langle \Phi_{N+1,M}(\mathbf{j}, \boldsymbol{\lambda}) | \Psi_\uparrow^\dagger(x, t) \Psi_\uparrow(y, t') | \Phi_{N+1,M}(\mathbf{j}, \boldsymbol{\lambda}) \rangle$.

2. Determinant representation for $\langle \Phi_{N,\bar{M}}(\mathbf{q}, \boldsymbol{\mu}) | \Psi_\uparrow(x, t) \Psi_\uparrow^\dagger(y, t') | \Phi_{N,\bar{M}}(\mathbf{q}, \boldsymbol{\mu}) \rangle$

In the case of the other type of mean value of bilocal operators $B = \langle \Phi_{N,\bar{M}}(\mathbf{q}, \boldsymbol{\mu}) | \Psi_\uparrow(x, t) \Psi_\uparrow^\dagger(y, t') | \Phi_{N,\bar{M}}(\mathbf{q}, \boldsymbol{\mu}) \rangle$ we have ($\bar{M} = M$ for $\sigma = \uparrow$)

$$\begin{aligned}
B &= \sum_{\substack{j_1 < \cdots < j_{N+1} \\ \lambda_1 < \cdots < \lambda_M}} \mathcal{F}_{N,M}^{(\uparrow)}(\mathbf{j}, \boldsymbol{\lambda}; \mathbf{q}, \boldsymbol{\mu} | x, t) \overline{\mathcal{F}}_{N,M}^{(\uparrow)}(\mathbf{j}, \boldsymbol{\lambda}; \mathbf{q}, \boldsymbol{\mu} | y, t'), \\
&= \sum_{\substack{j_1 < \cdots < j_{N+1} \\ \lambda_1 < \cdots < \lambda_M}} \frac{e^{i(t-t')\mu_\uparrow}}{N^M (N+1)^M} |\det_M B_\uparrow(\boldsymbol{\lambda}, \boldsymbol{\mu})|^2 \det_{N+1} D(\mathbf{j}, \mathbf{q} | x, t) \overline{\det_{N+1} D(\mathbf{j}, \mathbf{q} | y, t')}. \tag{B18}
\end{aligned}$$

Like in the previous case the summation over j 's is independent on the summation over λ 's and the summands are independently symmetric in j 's and λ 's and vanish when two of them are equal. Therefore, the summation can be written as

$$\sum_{\substack{j_1 < \cdots < j_{N+1} \\ \lambda_1 < \cdots < \lambda_M}} = \frac{1}{(N+1)!} \sum_{j_1=1}^{\infty} \cdots \sum_{j_{N+1}=1}^{\infty} \frac{1}{M!} \sum_{\lambda_1} \cdots \sum_{\lambda_M}, \tag{B19}$$

where $\sum_{\lambda} h(\lambda) = \sum_{l=1}^{N+1} h(\lambda_l)$ with $\lambda_l = \frac{2\pi}{N+1} \left(-\frac{N+1}{2} - \frac{1+(-1)^{N-M+1}}{4} + l \right)$ for an arbitrary function h .

a. *Summation over $\lambda_1, \dots, \lambda_{N+1}$*

The summation over the λ 's in (B18) can be written as

$$\begin{aligned}
B_j &= \frac{1}{(N+1)!} \sum_{j_1=1}^{\infty} \cdots \sum_{j_{N+1}=1}^{\infty} \det_{N+1} D(\mathbf{j}, \mathbf{q}|x, t) \overline{\det_{N+1} D(\mathbf{j}, \mathbf{q}|y, t')}, \\
&= \frac{1}{(N+1)!} \sum_{j_1=1}^{\infty} \cdots \sum_{j_{N+1}=1}^{\infty} \sum_{P, Q \in S_{N+1}} (-1)^{P+Q} \left(\prod_{l=1}^N f(j_{P(l)}, q_l|x, t) \bar{f}(j_{Q(l)}, q_l|y, t') \right) \phi_{j_{P(N+1)}}(x, t) \bar{\phi}_{j_{Q(N+1)}}(y, t'), \\
&= \frac{1}{(N+1)!} \sum_{j_1=1}^{\infty} \cdots \sum_{j_{N+1}=1}^{\infty} \sum_{R, Q \in S_{N+1}} (-1)^R \left(\prod_{l=1}^N f(j_{RQ(l)}, q_l|x, t) \bar{f}(j_{Q(l)}, q_l|y, t') \right) \phi_{j_{RQ(N+1)}}(x, t) \bar{\phi}_{j_{Q(N+1)}}(y, t'), \\
&= \frac{1}{(N+1)!} \sum_{j_1=1}^{\infty} \cdots \sum_{j_{N+1}=1}^{\infty} \sum_{Q \in S_{N+1}} \left(\prod_{l=1}^N \bar{f}(j_{Q(l)}, q_l|y, t') \right) \bar{\phi}_{j_{Q(N+1)}}(y, t') \\
&\quad \times \begin{vmatrix} f(j_{Q(1)}, q_1|x, t) & \cdots & f(j_{Q(1)}, q_N|x, t) & \phi_{j_{Q(1)}}(x, t) \\ \vdots & \ddots & \vdots & \vdots \\ f(j_{Q(N+1)}, q_1|x, t) & \cdots & f(j_{Q(N+1)}, q_N|x, t) & \phi_{j_{Q(N+1)}}(x, t) \end{vmatrix}. \tag{B20}
\end{aligned}$$

Multiplying the j -th row of the last determinant with $\bar{f}(j_{Q(j)}, q_j|y, t')$ and the $N+1$ -th row with $\bar{\phi}_{j_{Q(N+1)}}(y, t')$ we see that we have $j_{Q(l)}$ appearing only on the l -th row which means that we can sum inside the determinant. Introducing the \mathbf{q} dependent matrix and vectors

$$\tilde{U}_{ab}^{(+)}(x, t; y, t') = \sum_{j=1}^{\infty} f(j, q_b|x, t) \bar{f}(j, q_a|y, t'), \quad a, b = 1, \dots, N, \tag{B21}$$

$$\tilde{e}_a(x, t; y, t') = \sum_{j=1}^{\infty} f(j, q_a|x, t) \bar{\phi}_j(y, t'), \quad a = 1, \dots, N, \tag{B22}$$

$$\tilde{\bar{e}}_a(x, t; y, t') = \sum_{j=1}^{\infty} \bar{f}(j, q_a|y, t') \phi_j(x, t), \quad a = 1, \dots, N, \tag{B23}$$

and

$$g(x, t; y, t') = \sum_{j=1}^{\infty} \phi_j(x, t) \bar{\phi}_j(y, t'), \tag{B24}$$

then (B20) can be written as (the summation over the Q permutations gives $(N+1)!$ identical terms)

$$B_j = \begin{vmatrix} \tilde{U}_{1,1}^{(+)} & \cdots & \tilde{U}_{1,N}^{(+)} & \tilde{e}_1 \\ \vdots & \ddots & \vdots & \vdots \\ \tilde{U}_{N,1}^{(+)} & \cdots & \tilde{U}_{N,N}^{(+)} & \tilde{e}_N \\ \tilde{e}_1 & \cdots & \tilde{e}_N & g \end{vmatrix} (x, t; y, t'). \tag{B25}$$

Introducing the \mathbf{q} dependent matrix

$$\tilde{R}_{ab}^{(+)}(x, t; y, t') = \tilde{e}_a(x, t; y, t') \tilde{e}_b(x, t; y, t'), \quad a, b = 1, \dots, N, \tag{B26}$$

and expanding on the last column of (B25) we obtain

$$\begin{aligned}
B_j &= \left[g + \frac{\partial}{\partial z} \right] \det_N \left(\tilde{U}^{(+)} - z \tilde{R}^{(+)} \right), \\
&= \det_N \left(\tilde{U}^{(+)} - \tilde{R}^{(+)} \right) + (g-1) \det_N \tilde{U}^{(+)}. \tag{B27}
\end{aligned}$$

b. *Summation over $\lambda_1, \dots, \lambda_M$*

We have obtained that

$$B = \frac{1}{M!} \sum_{\lambda_1} \cdots \sum_{\lambda_M} \frac{e^{i(t-t')\mu_\uparrow}}{N^M(N+1)^M} |\det B_\uparrow(\boldsymbol{\lambda}, \boldsymbol{\mu})|^2 \left[\det_N \left(\tilde{U}^{(+)} - \tilde{R}^{(+)} \right) + (g-1) \det_N \tilde{U}^{(+)} \right], \quad (\text{B28})$$

where $\tilde{U}^{(+)}$ and $\tilde{R}^{(+)}$ depend on $\lambda_1, \dots, \lambda_M$ only via their sum $\Lambda = \lambda_1 + \dots + \lambda_M$. Like in the previous case this implies periodicity in Λ with period 2π . In this case $\Lambda = \frac{2\pi n}{N+1}$ with $n = 0, \dots, N$ which means that a resolution of identity is given by $1 = \sum_{m=0}^N \delta_{(N+1)} \left(m - (N+1) \frac{\lambda_1 + \dots + \lambda_M}{2\pi} \right)$ with

$$\delta_{(N+1)}(m) = \begin{cases} 1 & \text{if } m = 0 \pmod{N+1}, \\ 0 & \text{otherwise,} \end{cases} \quad \delta_{(N+1)}(m) = \frac{1}{N} \sum_{r=0}^N e^{\frac{2\pi i}{N} rm}, \quad (\text{B29})$$

Introducing $\tilde{U}_m^{(+)} = \tilde{U}^{(+)}|_{\Lambda=2\pi m/(N+1)}$ $\tilde{R}_m^{(+)} = \tilde{R}^{(+)}|_{\Lambda=2\pi m/(N+1)}$ the computations are similar with the ones in the previous section and [26] obtaining

$$B = e^{i(t-t')\mu_\uparrow} \frac{1}{N+1} \sum_{r,m=0}^N e^{\frac{2\pi i}{N+1} rm} \det_M O_r^{(+,\uparrow)} \left[\det_N \left(\tilde{U}_m^{(+)} - \tilde{R}_m^{(+)} \right) + (g-1) \det_N \tilde{U}_m^{(+)} \right], \quad (\text{B30})$$

with the $O_r^{(+,\uparrow)}$ matrices defined as (we correct a typo in 4.44 of [26])

$$[O_r^{(+,\uparrow)}]_{ab} = \frac{1}{N(N+1)} \sum_{m=1}^N \sum_{n=1}^N \sum_{\lambda} e^{-i(r+m-n)\lambda - im\mu_a + im\mu_b}, \quad a, b = 1, \dots, M. \quad (\text{B31})$$

3. Thermodynamic limit

The thermal summation in (17) and (18) is very similar with the one performed in [26] for two-component systems without an external potential (see also [30]). The main ingredient is the von Koch determinant formula which reads

$$\det(1 + zA) = 1 + z \sum_{m=1}^M A_{m,m} + \frac{z^2}{2!} \sum_{m=1}^M \sum_{n=1}^M \begin{vmatrix} A_{m,m} & A_{m,n} \\ A_{n,m} & A_{n,n} \end{vmatrix} + \dots \quad (\text{B32})$$

for A a square matrix of dimension M (which can also be infinite) and z a bounded complex parameter. Following the similar steps in [26] one obtains (32) and (34).

Appendix C: Thermodynamics of the impenetrable Gaudin-Yang model

In this Appendix we present some results for the thermodynamics of the trapped impenetrable Gaudin-Yang model. The energy spectrum of the trapped impenetrable system is given by (12). We notice two important features: a) it is independent of the statistics of the constituent particles and b) does not depend on the spin state $\boldsymbol{\lambda}$. This means that for the system with N particles of which M have spin down there are C_M^N states with the same energy for a given set of orbital numbers \boldsymbol{q} . The partition function is

$$\begin{aligned} \mathcal{Z}(\mu, B, T) &= \text{Tr} \left[e^{-H_I/T} \right] = \sum_{N=0}^{\infty} \sum_{M=0}^N \sum_{q_1 < \dots < q_N} \sum_{\mu_1 < \dots < \mu_M} e^{-E_{N,M}(\boldsymbol{q})/T}, \\ &= \sum_{N=0}^{\infty} \sum_{M=0}^N \sum_{q_1 < \dots < q_N} \sum_{\mu_1 < \dots < \mu_M} e^{2BM/T} e^{-\sum_{i=1}^N (\epsilon(q_i) - \mu + B)/T}, \\ &= \sum_{N=0}^{\infty} \sum_{q_1 < \dots < q_N} \left(1 + e^{2B/T} \right)^N e^{-\sum_{i=1}^N (\epsilon(q_i) - \mu + B)/T}, \end{aligned}$$

$$\begin{aligned}
&= \sum_{N=0}^{\infty} \sum_{q_1 < \dots < q_N} (2 \cosh(B/T))^N e^{-\sum_{i=1}^N (\varepsilon(q_i) - \mu)/T}, \\
&= \prod_{q=1}^{\infty} \left(1 + 2 \cosh(B/T) e^{-(\varepsilon(q) - \mu)/T} \right)
\end{aligned} \tag{C1}$$

where we have used $\sum_{M=0}^N \sum_{\mu_1 < \dots < \mu_M} e^{2BM/T} = \sum_{M=0}^N C_M^N e^{2B/T} = (1 + e^{2B/T})^N$. The grandcanonical potential $\phi(\mu, B, T) = U - TS - \mu(N_{\uparrow} + N_{\downarrow}) + B(N_{\uparrow} - N_{\downarrow})$ is

$$\phi(\mu, B, T) = -T \ln \mathcal{Z}(\mu, B, T) = -T \sum_{q=1}^{\infty} \ln \left(1 + 2 \cosh(B/T) e^{-(\varepsilon(q) - \mu)/T} \right). \tag{C2}$$

From the grandcanonical potential the number of particles of each type can be obtained as

$$N_{\uparrow} = -\frac{1}{2} \left(\frac{\partial \phi}{\partial \mu} - \frac{\partial \phi}{\partial B} \right) = \sum_{q=1}^{\infty} \frac{e^{-B/T}}{2 \cosh(B/T) + e^{(\varepsilon(q) - \mu)/T}}, \tag{C3}$$

$$N_{\downarrow} = -\frac{1}{2} \left(\frac{\partial \phi}{\partial \mu} + \frac{\partial \phi}{\partial B} \right) = \sum_{q=1}^{\infty} \frac{e^{B/T}}{2 \cosh(B/T) + e^{(\varepsilon(q) - \mu)/T}}. \tag{C4}$$

Appendix D: Elements of the $V^{(T,-)}$ matrix in the equal-time case

Here we derive the simplified expressions for the elements of the $V^{(T,-)}$ matrix in the equal-time case (41). Because $[V^{(T,-)}]_{ab} = \sqrt{\vartheta(a)}(U_{ab}^{(-)} - \delta_{a,b})\sqrt{\vartheta(b)}$ we will focus on $U_{ab}^{(-)}$ which is defined in (33a). We obtain different results depending on the ordering of x and y . In the case $x \leq y$ using (30) we have

$$\begin{aligned}
[U^{(-)}]_{ab} &= \delta_{a,b} - \zeta \int_y^{L_+} \bar{\phi}_a(w, t) \phi_b(w, t) dw - \bar{\zeta} \int_x^{L_+} \bar{\phi}_a(v, t) \phi_b(v, t) dv \\
&\quad + \zeta \bar{\zeta} \sum_{q=1}^{\infty} \left(\int_x^{L_+} \bar{\phi}_a(v, t) \phi_q(v, t) dv \right) \left(\int_y^{L_+} \bar{\phi}_q(w, t) \phi_b(w, t) dw \right), \\
&= \delta_{a,b} - \bar{\zeta} \int_x^y \bar{\phi}_a(v, t) \phi_b(v, t) dv - \underbrace{(\zeta + \bar{\zeta}) \int_y^{L_+} \bar{\phi}_a(w, t) \phi_b(w, t) dw}_A \\
&\quad + \underbrace{\zeta \bar{\zeta} \sum_{q=1}^{\infty} \left(\int_x^y \bar{\phi}_a(v, t) \phi_q(v, t) dv \right) \left(\int_y^{L_+} \bar{\phi}_q(w, t) \phi_b(w, t) dw \right)}_B \\
&\quad + \underbrace{\zeta \bar{\zeta} \sum_{q=1}^{\infty} \left(\int_y^{L_+} \bar{\phi}_a(v, t) \phi_q(v, t) dv \right) \left(\int_y^{L_+} \bar{\phi}_q(w, t) \phi_b(w, t) dw \right)}_C,
\end{aligned} \tag{D1}$$

with $\zeta = (1 - e^{i(\pi\kappa - \eta)})$. Now we will show that in the previous expression the terms A and C are equal cancelling each other. We have

$$\int_y^{L_+} \bar{\phi}_a(w, t) \phi_b(w, t) dw = \int_{L_-}^{L_+} \bar{\phi}_a(w, t) \tilde{\phi}_b(w, t) dw \tag{D2}$$

where $\tilde{\phi}_a(w, t) = \mathbf{1}_{[y, L_+]} \phi_a(w, t)$ and $\tilde{\phi}_b(w, t) = \mathbf{1}_{[y, L_+]} \phi_b(w, t)$ with $\mathbf{1}_{[y, L_+]}$ the characteristic function of the interval $[y, L_+]$ which is 1 when w is in the interval and 0 otherwise. Also, using the orthonormality of the wavefunctions (40) we find

$$\int_{L_-}^{L_+} \bar{\phi}_a(w, t) \tilde{\phi}_b(w, t) dw = \int_{L_-}^{L_+} \int_{L_-}^{L_+} \bar{\phi}_a(v, t) \delta(v - w) \tilde{\phi}_b(w, t) dw dv,$$

$$\begin{aligned}
&= \sum_{q=1}^{\infty} \left(\int_{L-}^{L+} \bar{\phi}_a(v, t) \phi_q(v, t) dv \right) \left(\int_{L-}^{L+} \bar{\phi}_q(w, t) \bar{\phi}_b(w, t) dw \right), \\
&= \sum_{q=1}^{\infty} \left(\int_y^{L+} \bar{\phi}_a(v, t) \phi_q(v, t) dv \right) \left(\int_y^{L+} \bar{\phi}_q(w, t) \phi_b(w, t) dw \right). \tag{D3}
\end{aligned}$$

Eqs. (D2) and (D3) together with $\zeta + \bar{\zeta} = \zeta \bar{\zeta} = 2 - 2 \cos(\pi\kappa - \eta)$ show that the A and C terms cancel each other in (D1). In a similar fashion it can be shown that $B = 0$ by noticing that it is the expansion of $\int_{L-}^{L+} \bar{\phi}_a(w, t) \bar{\phi}_b(w, t) dw$ with $\bar{\phi}_a(w, t) = \mathbf{1}_{[x, y]} \phi_a(w, t)$ and $\bar{\phi}_b(w, t) = \mathbf{1}_{[y, L+]} \phi_b(w, t)$ and $\mathbf{1}_{[x, y]} \mathbf{1}_{[y, L+]} = 0$. Therefore, we find

$$[V^{(T, -)}]_{ab} = - \left(1 - e^{-i[\pi\kappa - \eta]} \right) \sqrt{\vartheta(a)\vartheta(b)} \int_x^y \bar{\phi}_a(v, t) \phi_b(v, t) dv, \quad x \leq y. \tag{D4}$$

In the other case we obtain

$$[V^{(T, -)}]_{ab} = - \left(1 - e^{+i[\pi\kappa - \eta]} \right) \sqrt{\vartheta(a)\vartheta(b)} \int_y^x \bar{\phi}_a(v, t) \phi_b(v, t) dv, \quad y < x. \tag{D5}$$

Appendix E: Equivalence with Lenard's formula

We will show the equivalence of the determinant representation (43) with Lenard's formula (46). Similar with the particular case of zero temperature treated in Sec. VI the representation (46) can be understood as the first Fredholm minor of the integral operator $1 - \xi \hat{g}_\uparrow^{FF}$ acting on $[x, y]$ with kernel $g_\uparrow^{FF}(x, y|t) = \sum_{a=1}^{\infty} \vartheta(a) \bar{\phi}_a(x, t) \phi_a(y, t)$ and ξ defined in (47). From Hurwitz formula [89] we have

$$g_\uparrow^{(-)}(x, y|t) = R_\uparrow^{FF}(x, y|t) \det(1 - \xi \hat{g}_\uparrow^{FF}), \tag{E1}$$

with the resolvent satisfying the integral equation

$$R_\uparrow^{FF}(\lambda, \mu|t) = g_\uparrow^{FF}(\lambda, \mu|t) + \xi \int_x^y g_\uparrow^{FF}(\lambda, \nu|t) R_\uparrow^{FF}(\nu, \mu|t) d\nu. \tag{E2}$$

We will show that (43) is equivalent with (E1) but, first we need a preliminary result. For any invertible matrix A and two column vectors of the same dimension, u and v , the following identity holds: $\det(A + uv^T) = \det A + \det Av^T A^{-1}u$ [112]. Introducing $\phi_a^T(x, t) = \sqrt{\vartheta(a)} \phi_a(x, t)$ and noticing that the matrix $r^{(T, -)}$ defined in (44b) can be written as uv^T with $u = (\bar{\phi}_1^T(x, t), \bar{\phi}_2^T(x, t), \dots)^T$ and $v = (\phi_1^T(y, t), \phi_2^T(y, t), \dots)^T$ we find from (43)

$$g_\uparrow^{(-)}(x, y|t) = \det(1 + v^{(T, -)}) \sum_{i,j} \phi_i^T(y, t) \left[\left(1 + v^{(T, -)} \right)^{-1} \right]_{ij} \bar{\phi}_j^T(x, t). \tag{E3}$$

The proof that $\det(1 + v^{(T, -)}) = \det(1 - \xi \hat{g}_\uparrow^{FF})$ is the same as in Sec. V.B of [38]. It remains to show that the other term in the right hand side of (E3) is equal to $R_\uparrow^{FF}(x, y|t)$. In terms of ϕ_a^T we have $g_\uparrow^{FF}(\lambda, \mu|t) = \sum_{a=1}^{\infty} \bar{\phi}_a^T(\lambda, t) \phi_a^T(\mu, t)$. Plugging this in the equation for the resolvent (E2) we find

$$R_\uparrow^{FF}(\lambda, \mu|t) = \sum_{b=1}^{\infty} \bar{\phi}_b^T(\lambda, t) \phi_b^T(\mu, t) + \xi \sum_{b=1}^{\infty} \bar{\phi}_b^T(\lambda, t) B_b(\mu, t), \tag{E4}$$

with $B_b(\mu, t) = \int_x^y \phi_b^T(\nu, t) R_\uparrow^{FF}(\nu, \mu|t) d\nu$. In order to obtain the $B_b(\mu, t)$ coefficients we multiply the previous expression with $\phi_a^T(\lambda, t)$ and integrate from x to y . We obtain

$$B_a(\mu, t) = \sum_{b=1}^{\infty} A_{ba}(t) \phi_b^T(\mu, t) + \xi \sum_{b=1}^{\infty} A_{ba}(t) B_b(\mu, t), \tag{E5}$$

where we have introduced the matrix A with elements

$$A_{ab}(t) = \int_x^y \bar{\phi}_a^T(\lambda, t) \phi_b^T(\lambda, t) d\lambda. \tag{E6}$$

In terms of the column vectors $\phi = (\phi_1^T(\mu, t), \phi_2^T(\mu, t), \dots)^T$, $B = (B_1(\mu, t), B_2(\mu, t), \dots)^T$ the equation (E5) can be written as $B = A^T \phi + \xi A^T B$ with the solution $B = (1 - \xi A^T)^{-1} A^T \phi$. Using this result and (E4) we have $R_{\uparrow}^{FF}(\lambda, \mu|t) = \bar{\phi}^T \left(1 + \xi (1 - \xi A^T)^{-1} A^T\right) \phi$ with $\bar{\phi}^T = (\bar{\phi}_1^T(\lambda, t), \bar{\phi}_2^T(\lambda, t), \dots)$ a row vector. This last relation can also be written as $R_{\uparrow}^{FF}(\lambda, \mu|t) = \bar{\phi}^T (1 - \xi A^T)^{-1} \phi$ and shows that

$$R_{\uparrow}^{FF}(x, y|t) = \sum_{i,j} \bar{\phi}_i^T(x, t) \left[(1 - \xi A^T)^{-1} \right]_{ij} \phi_j^T(y, t). \quad (\text{E7})$$

Using $(1 - \xi A^T)^{-1} = \left[(1 - \xi A)^{-1} \right]^T$ this shows that (E7) is equal to the second term in the right hand side of (E3) proving the equivalence of the representations (46) and (43).

-
- [1] X.-W. Guan, M.T. Batchelor, and C. Lee, *Fermi gases in one dimension: From Bethe ansatz to experiments*, Rev. Mod. Phys. **85**, 1633 (2013).
- [2] M.A. Cazalilla, R. Citro, T. Giamarchi, E. Orignac, and M. Rigol, *One dimensional bosons: From condensed matter systems to ultracold gases*, Rev. Mod. Phys. **83**, 1405 (2011).
- [3] S.I. Mistakidis, A.G. Volosniev, R.E. Barfknecht, T. Fogarty, Th. Busch, A. Foerster, P. Schmelcher, N.T. Zinner, *Cold atoms in low dimensions – a laboratory for quantum dynamics*, arXiv:2202.11071.
- [4] T. Kinoshita, T. Wenger, and D. S. Weiss, *A quantum Newton's cradle*, Nature (London) **440**, 900 (2006).
- [5] M. Rigol, V. Dunjko, and M. Olshanii, *Thermalization and its mechanism for generic isolated quantum systems*, Nature (London) **452**, 854 (2008).
- [6] J.-S. Caux and F.H.L. Essler, *Time Evolution of Local Observables After Quenching to an Integrable Model*, Phys. Rev. Lett. **110**, 257203 (2013).
- [7] J.-S. Caux, *The Quench Action*, J. Stat. Mech. (2016) 064006.
- [8] O.A. Castro-Alvaredo, B. Doyon, and T. Yoshimura, *Emergent Hydrodynamics in Integrable Quantum Systems Out of Equilibrium*, Phys. Rev. X **6**, 041065 (2016).
- [9] B. Bertini, M. Collura, J. De Nardis, and M. Fagotti, *Transport in Out-of-Equilibrium XXZ Chains: Exact Profiles of Charges and Currents*, Phys. Rev. Lett. **117**, 207201 (2016).
- [10] E. Ilievski and J. De Nardis, *Ballistic transport in the one-dimensional Hubbard model: The hydrodynamic approach*, Phys. Rev. B **96**, 081118(R) (2017).
- [11] M. Mestyán, B. Bertini, L. Piroli, and P. Calabrese, *Exact solution for the quench dynamics of a nested integrable system*, J. Stat. Mech. (2017) 083103.
- [12] P. Siegl, S. I. Mistakidis, and P. Schmelcher, *Many-body expansion dynamics of a Bose-Fermi mixture confined in an optical lattice*, Phys. Rev. A **97**, 053626 (2018).
- [13] Y. Zhang, L. Vidmar, and M. Rigol, *Quantum dynamics of impenetrable $SU(N)$ fermions in one-dimensional lattices*, Phys. Rev. A **99**, 063605 (2019).
- [14] S. Wang, X. Yin, Y.-Y. Chen, Y. Zhang, and X.-W. Guan, *Emergent ballistic transport of Bose-Fermi mixtures in one dimension*, J. Phys. A **53**, 464002 (2020).
- [15] S. Scopa, P. Calabrese, and L. Piroli, *Real-time spin-charge separation in one-dimensional Fermi gases from Generalized Hydrodynamics*, Phys. Rev. B **104**, 115423 (2021).
- [16] E. Tartaglia, P. Calabrese, and B. Bertini, *Real-Time Evolution in the Hubbard Model with Infinite Repulsion*, SciPost Phys. **12**, 028 (2022).
- [17] S. Scopa, P. Calabrese, and L. Piroli, *Generalized Hydrodynamics of the repulsive spin- $\frac{1}{2}$ Fermi gas*, Phys. Rev. B **106**, 134314 (2022).
- [18] S.S. Alam, T. Skaras, L. Yang, and H. Pu, *Dynamical Fermionization in One-Dimensional Spinor Quantum Gases*, Phys. Rev. Lett. **127**, 023002 (2021).
- [19] O.I. Pătu, *Dynamical fermionization in a one-dimensional Bose-Fermi mixture*, Phys. Rev. A **105**, 063309 (2022).
- [20] O.I. Pătu, *Dynamical Fermionization in One-Dimensional Spinor Gases at Finite Temperature*, Phys. Rev. Lett. **130**, 163201 (2023).
- [21] V.E. Korepin, N.M. Bogoliubov, and A.G. Izergin, *Quantum Inverse Scattering Method and Correlation Functions* (Cambridge University Press, Cambridge, 1993).
- [22] A. Lenard, *One-dimensional impenetrable bosons in thermal equilibrium*, J. Math. Phys. **7**, 1268 (1966).
- [23] V.E. Korepin and N.A. Slavnov, *The time dependent correlation function of an Impenetrable Bose gas as a Fredholm minor.I*, Comm. Math. Phys. **129**, 103 (1990).
- [24] O.I. Pătu, V.E. Korepin, and D.V. Averin, *One-dimensional impenetrable anyons in thermal equilibrium: II. Determinant representation for the dynamic correlation functions*, J. Phys. A **41**, 255205 (2008).
- [25] A. Berkovich and J. H. Lowenstein, *Correlation function of the one-dimensional Fermi gas in the infinite-coupling limit (repulsive case)*, Nucl. Phys. B **285**, 70 (1987).

- [26] A.G. Izergin and A.G. Pronko, *Temperature correlators in the two-component one-dimensional gas*, Nucl. Phys. B **520**, 594 (1998).
- [27] O.I. Păţu, *Correlation functions of one-dimensional strongly interacting two-component gases*, Phys. Rev. A **100**, 063635 (2019).
- [28] J. Settino, N. Lo Gullo, F. Plastina, and A. Minguzzi, *Exact Spectral Function of a Tonks-Girardeau Gas in a Lattice*, Phys. Rev. Lett. **126**, 065301 (2021).
- [29] Q.-W. Wang, *Exact dynamical correlations of hard-core anyons in one-dimensional lattices*, Phys. Rev. B **105**, 205143 (2022).
- [30] O.I. Păţu, *Exact spectral function of the Tonks-Girardeau gas at finite temperature*, Phys. Rev. A **106**, 053306 (2022).
- [31] P.J. Forrester, N.E. Frankel, T.M. Garoni, and N.S. Witte, *Finite one-dimensional impenetrable Bose systems: Occupation numbers*, Phys. Rev. A **67**, 043607 (2003).
- [32] T. Papenbrock, *Ground-state properties of hard-core bosons in one-dimensional harmonic traps*, Phys. Rev. A **67**, 041601(R) (2003).
- [33] G. Marmorini, M. Pepe, and P. Calabrese, *One-body reduced density matrix of trapped impenetrable anyons in one dimension*, J. Stat. Mech. (2016) 073106.
- [34] Y. Hao, *Ground-state properties of hard-core anyons in a harmonic potential*, Phys. Rev. A **93**, 063627 (2016).
- [35] R. Pezer and H. Buljan, *Momentum Distribution Dynamics of a Tonks-Girardeau Gas: Bragg Reflections of a Quantum Many-Body Wave Packet*, Phys. Rev. Lett. **98**, 240403 (2007).
- [36] A. del Campo, *Fermionization and bosonization of expanding one-dimensional anyonic fluids*, Phys. Rev. A **78**, 045602 (2008).
- [37] Y.Y. Atas, D.M. Gangardt, I. Bouchoule, and K.V. Kheruntsyan, *Exact nonequilibrium dynamics of finite temperature Tonks-Girardeau gases*, Phys. Rev. A **95**, 043622 (2017).
- [38] O.I. Păţu, *Nonequilibrium dynamics of the anyonic Tonks-Girardeau gas at finite temperature*, Phys. Rev. A **102**, 043303 (2020).
- [39] P.J. Forrester, N.E. Frankel, T.M. Garoni, and N.S. Witte, *Painlevé transcendent evaluations of finite system density matrices for 1d impenetrable Bosons*, Commun. Math. Phys. **238**, 257 (2003).
- [40] Y.Y. Atas, I. Bouchoule, D.M. Gangardt, and K.V. Kheruntsyan, *Collective many-body bounce in the breathing mode oscillations of a Tonks-Girardeau gas*, Phys. Rev. A **96**, 041605(R) (2017).
- [41] W. Florkowski, M.P. Heller, and M. Spaliński, *New theories of relativistic hydrodynamics in the LHC era*, Rep. Prog. Phys. **81**, 046001 (2018).
- [42] Y. Le, Y. Zhang, S. Gopalakrishnan, M. Rigol, and D.S. Weiss, *Observation of hydrodynamization and local prethermalization in 1D Bose gases*, Nature **618**, 494 (2023).
- [43] M. Gaudin, *Un système a une dimension de fermions en interaction*, Phys. Lett. A **24**, 55 (1967).
- [44] C.N. Yang, *Some Exact Results for the Many-Body Problem in One Dimension with Repulsive Delta-Function Interaction*, Phys. Rev. Lett. **19**, 1312 (1967).
- [45] A. Kundu, *Exact Solution of Double δ Function Bose Gas through an Interacting Anyon Gas*, Phys. Rev. Lett. **83**, 1275 (1999).
- [46] M.D. Girardeau, *Anyon-Fermion Mapping and Applications to Ultracold Gases in Tight Waveguides*, Phys. Rev. Lett. **97**, 100402 (2006).
- [47] M.T. Batchelor, X.-W. Guan, and N. Oelkers, *One-Dimensional Interacting Anyon Gas: Low-Energy Properties and Haldane Exclusion Statistics*, Phys. Rev. Lett. **96**, 210402 (2006).
- [48] M.T. Batchelor and X.-W. Guan, *Generalized exclusion statistics and degenerate signature of strongly interacting anyons*, Phys. Rev. B **74**, 195121 (2006).
- [49] D.V. Averin and J.A. Nesteroff, *Coulomb Blockade of Anyons in Quantum Antidots*, Phys. Rev. Lett. **99**, 096801 (2007).
- [50] O.I. Păţu, V. E. Korepin, and D. V. Averin, *Correlation functions of one-dimensional Lieb-Liniger anyons*, J. Phys. A **40**, 14963 (2007).
- [51] P. Calabrese and M. Mintchev, *Correlation functions of one-dimensional anyonic fluids*, Phys. Rev. B **75**, 233104 (2007).
- [52] P. Calabrese and R. Santachiara, *Off-diagonal correlations in one-dimensional anyonic models: A replica approach*, J. Stat. Mech (2009) P03002.
- [53] Y. Hao, Y. Zhang, and S. Chen, *Ground-state properties of hard-core anyons in one-dimensional optical lattices*, Phys. Rev. A **79**, 043633 (2009).
- [54] T. Keilmann, S. Lanzmich, I. McCulloch, and M. Roncaglia, *Statistically induced phase transitions and anyons in 1D optical lattices*, Nat. Commun. **2**, 361 (2011).
- [55] Y. Hao and S. Chen, *Dynamical properties of hard-core anyons in one-dimensional optical lattices*, Phys. Rev. A **86**, 043631 (2012).
- [56] T.M. Wright, M. Rigol, M.J. Davis, and K.V. Kheruntsyan, *Nonequilibrium Dynamics of One-Dimensional Hard-Core Anyons Following a Quench: Complete Relaxation of One-Body Observables*, Phys. Rev. Lett. **113**, 050601 (2014).
- [57] J. Arcila-Forero, R. Franco, and J. Silva-Valencia, *Critical points of the anyon-Hubbard model*, Phys. Rev. A **94**, 013611 (2016).
- [58] L. Piroli and P. Calabrese, *Exact dynamics following an interaction quench in a one-dimensional anyonic gas*, Phys. Rev. A **96**, 023611 (2017).
- [59] S. Scopa, L. Piroli, and P. Calabrese, *One-particle density matrix of a trapped Lieb-Liniger anyonic gas*, J. Stat. Mech. (2020) 093103.

- [60] L. Piroli, S. Scopa, and P. Calabrese, *Determinant formula for the field form factor in the anyonic Lieb–Liniger model*, J. Phys. A **53**, 405001 (2020).
- [61] N.L. Harshman and A.C. Knapp, *Anyons from three-body hard-core interactions in one dimension*, Ann. Phys. **412**, 168003 (2020).
- [62] M. Bonkhoff, K. Jägering, S. Eggert, A. Pelster, M. Thorwart, and T. Posske, *Bosonic Continuum Theory of One-Dimensional Lattice Anyons*, Phys. Rev. Lett. **126**, 163201 (2021).
- [63] N.M. Myers and S. Deffner, *Thermodynamics of Statistical Anyons*, PRX Quantum **2**, 040312 (2021).
- [64] Y. Zhuravlev, E. Naichuk, N. Iorgov, and O. Gamayun, *Large-time and long-distance asymptotics of the thermal correlators of the impenetrable anyonic lattice gas*, Phys. Rev. B **105**, 085145 (2022).
- [65] A. Osterloh, L. Amico, and U. Eckern, *Bethe Ansatz solution of a new class of Hubbard-type models*, J. Phys. A **33**, L87 (2000).
- [66] M.T. Batchelor, A. Foerster, X.-W. Guan, J. Links, and H.-Q. Zhou, *Quantum inverse scattering method with anyonic grading*, J. Phys. A **41**, 465201 (2008).
- [67] Y.-L. Yao, J.-P. Cao, G.-L. Li, and H. Fan, *Exact solutions of a multi-component anyon model with SU(N) invariance*, J. Phys. A **45**, 045207 (2012).
- [68] R.A. Santos, F.N.C. Paraan, and V.E. Korepin, *Quantum phase transition in a multicomponent anyonic Lieb–Liniger model*, Phys. Rev. B **86**, 045123 (2012).
- [69] N.T. Zinner, *Strongly interacting mesoscopic systems of anyons in one dimension*, Phys. Rev. A **92**, 063634 (2015); **93**, 049901(E) (2016).
- [70] L. Cardarelli, S. Greschner, and L. Santos, *Engineering interactions and anyon statistics by multicolor lattice depth modulations*, Phys. Rev. A **94**, 023615 (2016).
- [71] F. Colomo, A. G. Izergin, V. E. Korepin, and V. Tognetti, *Temperature correlation functions in the XX0 Heisenberg chain. I*, Theor. Math. Phys. **94**, 11 (1993).
- [72] M. Ogata and H. Shiba, *Bethe-ansatz wave function, momentum distribution, and spin correlation in the one-dimensional strongly correlated Hubbard model*, Phys. Rev. B **41**, 2326 (1990).
- [73] F.H.L. Essler, H. Frahm, F. Göhmann, A. Klümper, and V.E. Korepin, *The One-Dimensional Hubbard Model* (Cambridge University Press, Cambridge, England, 2005).
- [74] F. Deuretzbacher, K. Fredenhagen, D. Becker, K. Bongs, K. Sengstock, and D. Pfannkuche, *Exact Solution of Strongly Interacting Quasi-One-Dimensional Spinor Bose Gases* Phys. Rev. Lett. **100**, 160405 (2008).
- [75] L. Guan, S. Chen, Y. Wang, and Z. Q. Ma, *Exact Solution for Infinitely Strongly Interacting Fermi Gases in Tight Waveguides*, Phys. Rev. Lett. **102**, 160402 (2009).
- [76] A.G. Volosniev, D.V. Fedorov, A.S. Jensen, M. Valiente, and N.T. Zinner, *Strongly interacting confined quantum systems in one dimension*, Nat. Commun. **5**, 5300 (2014).
- [77] J. Levinsen, P. Massignan, G.M. Bruun, and M.M. Parish, *Strong-coupling ansatz for the one-dimensional Fermi gas in a harmonic potential*, Sci. Adv. **1**, e1500197 (2015).
- [78] L. Yang and X. Cui, *Effective spin-chain model for strongly interacting one-dimensional atomic gases with an arbitrary spin*, Phys. Rev. A **93**, 013617 (2016).
- [79] F. Deuretzbacher, D. Becker, J. Bjerlin, S.M. Reimann, and L. Santos, *Spin-chain model for strongly interacting one-dimensional Bose-Fermi mixtures*, Phys. Rev. A **95**, 043630 (2017).
- [80] L. Yang, S.S. Alam, and H. Pu, *Generalized Bose–Fermi mapping and strong coupling ansatz wavefunction for one dimensional strongly interacting spinor quantum gases*, J. Phys. A **55**, 464005 (2022).
- [81] O. Gamayun, E. Quinn, K. Bidzhiev, and M.B. Zvonarev, *Emergence of anyonic correlations from spin and charge dynamics in one dimension*, arXiv:2301.02164.
- [82] A. Berkovich, *Temperature and magnetic field-dependent correlators of the exactly integrable (1+1)-dimensional gas of impenetrable fermions*, J. Phys. A **24**, 1543 (1991).
- [83] V.V. Cheianov and M.B. Zvonarev, *Nonunitary Spin-Charge Separation in a One-Dimensional Fermion Gas*, Phys. Rev. Lett. **92**, 176401 (2004).
- [84] V.V. Cheianov and M.B. Zvonarev, *Zero temperature correlation functions for the impenetrable fermion gas*, J. Phys. A **37**, 2261 (2004).
- [85] V.V. Cheianov, H. Smith, and M.B. Zvonarev, *Low-temperature crossover in the momentum distribution of cold atomic gases in one dimension*, Phys. Rev. A **71**, 033610 (2005).
- [86] K.A. Matveev, *Conductance of a Quantum Wire in the Wigner-Crystal Regime*, Phys. Rev. Lett. **92**, 106801 (2004).
- [87] G.A. Fiete and L. Balents, *Green’s Function for Magnetically Incoherent Interacting Electrons in One Dimension*, Phys. Rev. Lett. **93**, 226401 (2004).
- [88] G.A. Fiete, *Colloquium: The spin-incoherent Luttinger liquid*, Rev. Mod. Phys. **79**, 801 (2007).
- [89] W.A. Hurwitz, *Note on the Fredholm determinant*, Bull. Am. Math. Soc. **20**, 406 (1914).
- [90] C.A. Tracy and H. Widom, *Fredholm determinants, differential equations and matrix models*. Commun. Math. Phys. **163**, 33 (1994).
- [91] N.S. Witte, P.J. Forrester, and C.M. Cosgrove, *Gap probabilities for edge intervals in finite Gaussian and Jacobi unitary matrix ensembles*. Nonl. **13**, 1439 (2000).
- [92] V.S. Popov and A.M. Perelomov, *Parametric excitation of a quantum oscillator II*, Zh. Eksp. Teor. Fiz. **57**, 1684 (1970) [JETP **30**, 910 (1970)].
- [93] A.M. Perelomov and Y. B. Zel’dovich, *Quantum Mechanics: Selected Topics* (World Scientific, Singapore, 1998).

- [94] M. Rigol and A. Muramatsu, *Fermionization in an Expanding 1D Gas of Hard-Core Bosons*, Phys. Rev. Lett. **94**, 240403 (2005).
- [95] A. Minguzzi and D.M. Gangardt, *Exact Coherent States of a Harmonically Confined Tonks-Girardeau Gas*, Phys. Rev. Lett. **94**, 240404 (2005).
- [96] D.M. Gangardt and M. Pustilnik, *Correlations in an expanding gas of hard-core bosons*, Phys. Rev. A **77**, 041604(R) (2008).
- [97] J.-S. Caux, B. Doyon, J. Dubail, R. Konik, and T. Yoshimura, *Hydrodynamics of the interacting Bose gas in the Quantum Newton Cradle setup*, SciPost Phys. **6**, 070 (2019).
- [98] C.J. Bolech, F. Heidrich-Meisner, S. Langer, I.P. McCulloch, G. Orso, and M. Rigol, *Long-Time Behavior of the Momentum Distribution During the Sudden Expansion of a Spin-Imbalanced Fermi Gas in One Dimension*, Phys. Rev. Lett. **109**, 110602 (2012).
- [99] A.S. Campbell, D.M. Gangardt, and K.V. Kheruntsyan, *Sudden Expansion of a One-Dimensional Bose Gas from Power-Law Traps*, Phys. Rev. Lett. **114**, 125302 (2015).
- [100] W. Xu and M. Rigol, *Expansion of one-dimensional lattice hard-core bosons at finite temperature*, Phys. Rev. A **95**, 033617 (2017).
- [101] J.M. Wilson, N. Malvania, Y. Le, Y. Zhang, M. Rigol, and D. S. Weiss, *Observation of dynamical fermionization*, Science **367**, 1461 (2020).
- [102] B. Fang, G. Carleo, A. Johnson, and I. Bouchoule, *Quench-Induced Breathing Mode of One-Dimensional Bose Gases*, Phys. Rev. Lett. **113**, 035301 (2014); **116**, 169901(E) (2016).
- [103] R. van den Berg, B. Wouters, S. Eliëns, J. De Nardis, R.M. Konik, and J.-S. Caux, *Separation of Time Scales in a Quantum Newton's Cradle*, Phys. Rev. Lett. **116**, 225302 (2016).
- [104] P. Meystre, *Atom Optics* (Springer, Germany, 2009) Chap. 4.
- [105] B. Dubetsky and P.R. Berman, *Atom Gratings Produced by Large-Angle Atom Beam Splitters*, Phys. Rev. A **64**, 063612 (2001).
- [106] M. Schemmer, I. Bouchoule, B. Doyon, and J. Dubail, *Generalized Hydrodynamics on an Atom Chip*, Phys. Rev. Lett. **122**, 090601 (2019).
- [107] K.F. Thomas, M.J. Davis, and K.V. Kheruntsyan, *Thermalization of a quantum Newton's cradle in a one-dimensional quasicondensate*, Phys. Rev. A **103**, 023315 (2021).
- [108] H.G. Vaidya and C.A. Tracy, *One-Particle Reduced Density Matrix of Impenetrable Bosons in One Dimension at Zero Temperature*, Phys. Rev. Lett. **42**, 3 (1979).
- [109] H.G. Vaidya and C.A. Tracy, *One-particle reduced density matrix of impenetrable bosons in one dimension at zero temperature*, J. Math. Phys. **20**, 2291 (1979).
- [110] M. Jimbo, T. Miwa, Y. Mori and M. Sato, *Density matrix of an impenetrable Bose gas and the fifth Painlevé transcendent*, Physica D (Amsterdam) **1**, 80 (1980).
- [111] D.M. Gangardt, *Universal correlations of trapped one-dimensional impenetrable bosons*, J. Phys. A **37**, 9335 (2004).
- [112] M. Marcus, *Determinants of sums*, College Math. J. **21**, 130 (1990).